Received: 17 October 2018
接收日期：2018年10月17日
Revised: 17 December 2018
修订日期：2018年12月17日
Accepted: 19 December 2018
收录日期：2018年12月19日

DOI: 10.1002/jrs.5558
DOI:10.1002/jrs.5558

RESEARCH ARTICL E
研究论文E

WILEY Journal of RAMAN SPECTROSCOPY

The Raman signature of protonic species as a potential tool for dating or authentication of glazed pottery
釉陶定年或鉴定潜在工具——质子物质的拉曼信号

Burcu Kırmızı[1,2] | Stephen Chen [3] | Philippe Colomban [1]
Burcu Kırmızı[1,2] | 陈志宏 [3] | Philippe Colomban [1]

[1] Sorbonne Université, CNRS, MONARIS UMR 8233, Campus Pierre et - Marie Curie, Paris, France
1法国巴黎索邦大学皮埃尔和玛丽居里大学CNRS， MONARIS UMR 8233

[2] School of Conservation and Restoration of Movable Cultural Property, Mimar Sinan Fine Arts University, Istanbul, Turkey
2 土耳其伊斯坦布尔米玛•悉楠美术大学可移动文化遗产保护与修复学院

[3] Royal Heritage Ceramics Authentication Ltd., Shatin, Hong Kong
3 皇朝遗珍古陶瓷实验室，香港沙田

Correspondence
通讯地址
Philippe Colomban, Sorbonne Université, CNRS, MONARIS UMR 8233, Campus
Philippe Colomban，索邦大学CNRS，地址：MONARIS UMR 8233, Campus
Pierre et - Marie Curie, 4 Place Jussieu, 75005 Pa
Pierre et - Marie Curie, 4 Place Jussieu, 75005 Pa
Email: philippe.colomban@upmc.fr
电子邮箱：philippe.colomban@upmc.fr

Abstract
摘要

In this study, the potential of Raman spectroscopy is discussed for the comparative dating or authentication of glazed pottery based on the Raman signature of protonic species incorporated in the glazes due to the corrosion processes as a function of time, chemical composition, and environmental conditions. According to the literature and analyses on a reference set of glass samples that had previously been subjected to heavy corrosion in laboratory conditions and extensively studied by Infrared spectroscopy, the accumulation of protonic species such as water and hydroxyl groups on the surface of glassy silicates gives rise to a specific Raman signature in the 2,000–3,800 cm^{-1} range. The relative intensity of this Raman signature is mainly considered to act as a means of discriminating between old and modern artefacts. In order to check this hypothesis, glazed pottery with different origins (Chinese and Vietnamese stoneware or celadons, blue - and - white and painted enamelled porcelains, Islamic *terra cottas*) and different chemical compositions or processing conditions from a wide time span (~1000 to the present) were analysed by Raman microspectroscopy. Further comparative data was obtained by modifying the experimental parameters such as laser wavelength, objective magnification, and confocal hole. The results showed that Raman intensity of the protonic species shows a correlation with age for lead free glazed pottery in the case of celadons and porcelains. The intensity strongly depends on the chemical composition of the glaze as well as the preservation conditions to a certain degree.

本文基于釉料中质子物质的拉曼信号，讨论了采用拉曼光谱技术对釉陶进行比较定年和鉴定的潜力，认为釉中质子物质的拉曼信号的腐蚀过程随时间、化学成分和环境条件的变化而变化。根据文献资料、对一组参照玻璃样品（先前已在实验室条件下遭受严重腐蚀）的分析及通过红外光谱法进行的广泛研究可以得知，质子物质（例如水和羟基）在玻璃硅酸盐表面的积累在2,000-3,800cm^{-1}范围内会产生特定的拉曼信号。大体上，这种拉曼信号的相对强度被视为是鉴别古代和现代手工艺品的一种方法。为了验证这一假说，采用显微拉曼光谱技术对较长时间跨度内（～1000年至今）源自不同产地（中国和越南的炻瓷或青瓷、青花瓷和珐琅彩瓷、伊斯兰陶瓷），具有不同化学成分或加工条件的釉陶进行了拉曼光谱分析。通过修改诸如激光波长、物镜放大倍率和共聚焦孔等实验参数获得进一步的比较数据。结果表明，在青瓷和陶瓷中，无铅釉陶质子物质的拉曼光谱强度与年代有关。其强度很大程度上取决于釉料的化学成分及保存条件。

KEYWORDS
关键词
authentication, dating, glass corrosion, glazed pottery, water
鉴定，定年，玻璃腐蚀，釉陶，水

1 | INTRODUCTION
1 | 引言

Dating of ancient artefacts, especially the ones with inorganic composition (no carbon), has always been a focal point in archaeological and art historical studies, which consequently led to the development of several scientific methods for dating in the 20th century. Among these artefacts of inorganic origin, objects made of glassy silicates (natural and synthetic glasses, pottery glazes, enamels, etc.) have been one of the major interests in dating research for the last decades.

古代手工艺品，特别是无机成分（不含碳）的定年一直是考古学和艺术史研究的重点，并由此推动了20世纪几种科学定年方法的发展。在这些无机成因的手工艺品中，玻璃硅酸盐制品（天然和合成玻璃、陶瓷釉料、搪瓷等）在过去几十年里一直是定年研究的主要关注对象之一。

Given the fact that all glassy objects corrode in the course of time as a function of their chemical composition and environmental conditions, attempts have been made to date archaeological glasses on the basis of measuring the thickness of their corrosion layers formed as a function of time. [1] In terms of glass corrosion, it has been known for a very long time that the most important factor is the presence of (acidic) water in the environment. [2–6]

鉴于所有玻璃质物体在其化学成分和环境条件的作用下都会随着时间的推移而遭受腐蚀的事实，因此，在测量其随时间变化而形成的腐蚀层厚度的基础上，人们已尝试确定考古玻璃的年代。[1] 就玻璃腐蚀而言，众所周知，最重要的因素是环境中（酸性）水的存在。[2–6]

© 2019 John Wiley & Sons, Ltd.
© 2019 John Wiley&Sons, Ltd.

In that case, protonic species primarily tend to replace the alkali ions such as K^+, Na^+, Li^+, and Mg^{2+} in the glass network by their hydrogen ions (H^+ and/or H_3O^+) on the basis of an inter- diffusion process. The hydrogen ions, namely, the protons therefore cause the diffusion of these network modifiers out of the glass network, breaking some of the Si–O–Si links. This process also has mechanical effects on the glass due to the changes in the microstructure as a result of stress in the form of defects (microcracks and voids), [2,4,7,8] and it is expected that the number of these defects will be increased as a function of time and hence the reactivity of the glass is enhanced. The thickness of the so - called corroded layer will thus increase in a nonlinear way, leading to the possibility of dating or authentication of old artefacts.

在这种情况下，质子物质主要倾向于通过相互扩散过程中产生的氢离子（H +和/或 H_3O +）取代玻璃网络中的碱性离子，例如 K^+、Na^+、Li^+ 和 Mg^{2+}。因此，氢离子（即质子）会导致这些网络修饰体从玻璃网络中扩散出去，断开一些 Si–O–Si键。由于以缺陷（微裂纹和空隙）形式存在的应力导致微观结构发生变化，因此该过程对玻璃也有机械影响。[2,4,7,8]预计随着时间的推移，这些缺陷的数量会有所增加，从而增强玻璃的反应性。所谓腐蚀层的厚度因此会以非线性方式增加，从而有可能测定或鉴定古代手工艺品的年代。

Water molecules and hydroxyl groups are also adsorbed inside the (highly porous) corrosion layers as in the case of oxide surfaces [9–11] to saturate the dangling bonds and hence increases in the specific surface area will increase the amount of water molecules adsorbed.

水分子和羟基也会被吸附在（高孔隙度）腐蚀层中，例如在氧化物表面[9–11]使不饱和键饱和的情况下，因此，比表面积会增加，水分子的吸附量也会随之增加。

All of these species containing protons (including water) that react with glass form bonds at the molecular level by hydrogen bonding (either strong or weak). As a result, glass (and glaze) corrosion induces water, proton, and/or OH^- incorporation in the surface region of glassy silicates. This has been clearly demonstrated for potash stained glasses at the millimetre or submillimetre scale, both by Optical and Scanning Electron Microscopy, Thermogravimetry, and by Infrared and Raman spectroscopy. [7,8] A late study about the very surface analyses of rock crystal objects made up of quartz, a more stable type of silicate than man - made glass, by nuclear techniques also shows the time - dependent penetration of “hydrogen” in this very stable mineral but at the submicron scale. [12] The uptake of water from the environment as a function of time was also qualitatively observed in ancient obsidian [13] and quartz [14] artefacts.

所有这些含有质子的物质（包括水）通过氢键（强或弱）与分子水平的玻璃形成键反应。因此，玻璃（和釉）腐蚀会在玻璃硅酸盐表面区域诱导水、质子和/或 OH^- 结合。通过光学和扫描电子显微镜、热重分析以及红外和拉曼光谱技术在毫米或亚毫米级对钾彩色玻璃进行的测定已清楚地证明了这一点。[7,8] 利用核技术对石英(一种比人造玻璃更稳定的硅酸盐)构成的岩石晶体进行表面分析的最新研究也表明，“氢”在这种非常稳定的矿物中（但在亚微米尺度上）的渗透随时间的推移而变化。[12] 在古代黑曜石[13]和石英[14]手工艺品中，也定性地观察到从环境中吸收的水分随时间的变化。

Raman microspectroscopy is now a well - established technique for the characterization of covalently bonded compounds as those constituting ceramics and glass. Furthermore, mobile Raman set - up allows the fast identification of crystalline and amorphous phases in a nonintrusive way on - site [15] and use of the technique has also developed rapidly for the authentication of glass, pottery, and enamelled objects. [15–18] Raman spectroscopy is an optical technique, which is directly influenced by the optical properties of the materials analysed, such as transparency and colour. Transparency of a glass is very much affected by the presence of defects on the surface as well as some other surface - deposited materials as a result of corrosion processes. [19]

显微拉曼光谱技术现在是一项用于表征构成陶瓷和玻璃的共价键合化合物的成熟技术。此外，移动式拉曼装置允许在现场以非侵入性的方式快速识别晶相和非晶相[15]，而且该技术在玻璃、陶瓷和搪瓷制品的鉴定方面也得到了迅速发展。[15-18] 拉曼光谱技术是一种光学技术，直接受所分析材料的光学性质（如透明度和颜色）影响。由于腐蚀过程，玻璃的透明度受到表面上的缺陷以及一些其他表面沉积物质的严重影响。[19]

The selection of high magnification microscope objectives allows the specific analysis of the near surface of artefacts. It has been demonstrated that the absolute as - recorded Raman intensity (glass signature) at the surface of rather similar types of glass objects, which were preserved in the same or similar conditions decreases as a function of time and thus can be used for the purpose of comparative dating. [6,17] The identification of protonic species (water, hydroxyl groups, etc.) in glass can be performed by Raman spectroscopy but better by infrared (strong bands between 2,500 and 3,800 cm^{-1}) and near infrared (overtones and combination bands) absorption or reflexion methods [7,8,20,21] due to the strong dipolar character of X–H bonds. However, infrared methods require a flat, glossy surface, or a sample preparation procedure in the form of thin samples or powder dispersed in KBr or CsI solid pellets or in Nujol™ or Fluorolube™ mulls, which is destructive and time - consuming. The low intensity of the near infrared signature allows measuring the transmission through thick and optically clear (polished) samples (>mm). However, as a scattering technique, Raman spectroscopy requires no preparation of the sample. [15,16,19] Preliminary measurements have pointed out the presence of protonic species signature in the Raman spectrum of ancient glazed pottery recorded at the very surface. [16] Raman signature of the protonic species with weak, more or less broad features obtained in the 2,000– 3,800 cm^{-1} range, and their relative intensity could be used as a potential tool for the discrimination of old and modern artefacts, that is, genuine artefacts and copies or fakes and for the comparison of samples with an unknown age.

高放大倍率显微镜物镜的选择允许对手工艺品的近表面进行特定分析。已经证明，在相同或相似条件下保存的相当相似类型玻璃物体表面上记录的拉曼强度（玻璃特征）绝对值随时间的推移而降低，因此可用于比较定年。[6,17] 由于 X-H 键的强偶极特性，玻璃中的质子物质（水、羟基等）可通过拉曼光谱技术进行鉴别，但通过红外（2,500-3,800cm^{-1}之间的强谱带）和近红外（泛频和组合谱带）吸收或反射方法[7,8,20,21]进行鉴别效果更佳。然而，红外方法要求表面平坦、光滑，或将样品以薄样品或粉末形式制备，分散在KBr或CsI固体颗粒或Nujol™或Fluoroube™研磨机中，这是一种具有破坏性且耗时的样品制备方法。近红外信号的低强度允许测量通过厚且光学透明（抛光）样品（> mm）的透射率。然而，作为一种散射技术，拉曼光谱技术不需要制备样品。[15,16,19]初步测量指出，在古代釉陶表面记录的拉曼光谱中存在质子物质特征。[16]在2,000-3,800 cm^{-1} 范围内获得的具有较弱、较多或较少宽谱带特征的质子物质的拉曼信号及其相对强度可用作鉴别古代和现代手工艺品（即真品和复制品或仿制品），并与年代不详的样品进行比较的潜在工具。

In order to test the potential of this method, we present here a comparison of the Raman signals recorded on 20 glazed pottery of different origins (Chinese and Vietnamese stoneware or celadons, blue - and - white and painted enamelled porcelains, Islamic *terra cottas*) from different time periods (the beginning of the 11th century to the present, including modern fakes). The pottery samples were selected on the basis of their “conservation” history (excavated from soil or from shipwreck) and glaze compositions, hence different chemical resistance towards corrosion: high - melting temperature (T_m) porcelains (feldspar - based glaze), medium T_m stoneware or celadons (calcium - rich glaze) and low T_m *terra cottas* (lead - based glaze). Five different corroded glass pieces previously characterized by Raman, IR, and nIR spectroscopy [8] were also used as reference for the Raman signatures of the protonic species. The methodological procedure was also discussed with different experimental parameters such as laser wavelength, objective magnification, and confocal hole.

为了测试这种方法的潜力，本文比较了20种不同来源的釉陶（中国和越南的炻瓷或青瓷、青花瓷和珐琅彩瓷、伊斯兰陶瓷）在不同时期（11世纪初期到现在，包括现代仿制品）记录的拉曼信号。由于陶瓷样品是基于其“保存”历史（从土壤或沉船中出土）和釉料成分挑选的，因此这些样品对腐蚀有不同的耐化学性：高熔点（Tm）瓷器（长石釉）、中熔点炻瓷或青瓷（富钙釉）和低熔点瓷釉（铅基釉）。先前通过拉曼光谱、红外光谱和近红外光谱技术[8]对5种不同的腐蚀玻璃样品进行表征，并以此作为质子物质拉曼信号的参考。还讨论了激光波长、物镜放大倍率、共聚焦孔等不同实验参数对该方法的影响。

2 | EXPERIMENTAL | 实验

2.1 | Artefacts |手工艺品

The pottery samples were selected on the basis of three criteria, such as the age of the artefact, its glaze composition, and the environmental condition of its preservation (soil and sea) in order to be able to test our hypothesis. Thus, the samples belong to different types of glazed pottery coming from different cultures and belong to a wide time span from ca. 11th century up to the present time (fakes are also included, see Table 1). The reference samples were selected from a previous study on naturally (meteoric water) and artificially corroded (with H_2SO_4) pieces of stained glass windows (soda‐lime and potash‐lime glass), dating to the 13th–19th centuries. They had been obtained from ancient notable cathedrals in France, such as Le Mans and Amiens (Table 2). [8,22] A total of 25 samples were analysed, each of them at least at two to three spots.

为了验证我们的假设，我们根据手工艺品的年代、釉料成分和保存环境条件（土壤和海洋）三种标准来选择陶瓷样品。因此，这些样品都是较长时间跨度内（约11世纪至今）具有不同文化背景的不同类型的釉陶（也包括仿制品，见表1）。参考样品依据以前对自然（大气水）和人工腐蚀（H_2SO_4）彩色玻璃窗（碱石灰和钾钙玻璃）的研究加以选择，样品年代可追溯到13-19世纪。它们取自法国著名的古代大教堂，如勒芒和亚眠大教堂（表2）。[8,22]总共分析了25份样品，每份样品至少在两至三个地点进行分析。

The first group of samples consists of porcelains displaying different production techniques and mostly belonging to Chinese origin (Table 1 and Figure 1). The earliest Chinese porcelain samples are dated to the Ming Dynasty (1368–1644) and belong to the blue‐and‐white group with underglaze blue decoration. The selected samples along with other similar Chinese blue‐and‐whites have previously been studied (see previous studies [23–25] and references herein), in particular by Raman microspectroscopy. [23] The later Chinese porcelain samples belong to the different reigns of the Qing Dynasty (1644–1911) with multicolours and include different groups, such as *wucai*, *Famille Rose*, and *fencai*. These samples display a range of painting techniques with alkali‐ or earth‐alkali‐based glazes and lead‐based overglaze (yellow, red, etc.) painted decorations. Their detailed descriptions can be found in a very recent study. [26] The last Chinese porcelain sample is a modern fake of the Ming Dynasty blue‐and‐white. The other blue‐and‐white porcelain samples are of Vietnamese origin, dating to the Lê Dynasty from the 15th century that had been the period of commercial expansion of Vietnamese pottery to the world, taking advantage of the Ming embargo of exportation. The Vietnamese porcelain samples are products of the Chu Đau kilns from the north of Vietnam, which was one of the most important ceramic production centres during the 15th–16th centuries. [23,27–30] One of the shards had been recovered in the mid‐15th century Cu Lao Cham shipwreck that was found close to the commercial port of Hoi An in central Vietnam. [29] The excavations of the shipwreck conducted ~80 m undersea in the late 20th century had revealed a great quantity of Vietnamese ceramics. [27] These glazes have a lime‐potash aluminosilicate composition. [23,27]

第一组样品由展示不同生产工艺的瓷器组成，大部分来自中国（表1和图1）。中国最早的瓷器样品可以追溯到明朝（1368-1644年），属于采用釉里青装饰的青花瓷。先前已对所选样品及其他类似的中国青花瓷进行过研究（见先前的研究[23-25] 和本文的参考文献），特别是采用显微拉曼光谱技术进行了研究。[23]后续的中国瓷器样品属于清朝（1644-1911年）不同统治时期的瓷器，颜色多样，包括五彩、软彩、粉彩等不同类别。这些样品展示了一系列使用碱或土碱釉和铅基釉（黄色、红色等）彩绘装饰的彩绘技术。其详细描述可在最近开展的一项研究中找到。[26]最后一件中国瓷器样品是一件明朝青花瓷的现代仿制品。其他的青花瓷样品来自越南，样品年代可以追溯到15世纪的黎王朝，当时越南陶瓷正利用明朝的出口禁令向全世界进行商业扩张。越南瓷器样品出自越南北部的Chu Dau窑，该窑厂是15-16世纪最重要的陶瓷生产中心之一。[23,27-30]其中一块陶瓷碎片是于15世纪中叶在越南中部港口城市会安附近发现的Cu Lao Cham号沉船中找到的。[29] 20世纪末，在海底约80米处对该沉船进行挖掘，发现了大量越南陶瓷。[27]这些釉料含有石灰钾铝硅酸盐成分。[23,27]

Another category of samples consists of celadons or stoneware with mostly Vietnamese origin (Figures 2 and 3). The ancient Vietnamese samples are dated between the 12th–15th centuries (Ly and Lê Dynasties, Table 1). [18,27,30] Their glazes have a lime aluminosilicate composition, as in the case of Chinese and Korean celadons. [24,31] Most of the Vietnamese celadons or stoneware dating to the Ly Dynasty were produced in the Ha Lan kilns, which are situated in the southeast of Hanoi. [30] The 15th century Vietnamese celadon sample, a product of the Chu Đau kilns, also comes from the excavation of Cu Lao Cham shipwreck. [27,29] The modern Vietnamese celadon is a fake, which was produced in the Bat Trang kiln, a famous site always active close to Hanoi. This sample has already been analysed. [18] Other celadon samples are dated to the Southern Song Dynasty (1127–1279) in China and Goryeo Dynasty (918–1392) in Korea.
另一类样品由青瓷或炻瓷组成，大部分来自越南（图2和图3）。越南的古代样品可以追溯到12-15世纪（李朝和黎朝，表1）。[18,27,30]他们的釉料含有石灰铝硅酸盐成分，如中国和韩国的青瓷一样。[24,31] 越南青瓷或炻瓷大多可追溯到李朝，产于河内东南部的Ha Lan窑。[30] 15世纪越南青瓷样品，产自Chu Dau窑，由Cu Lao Cham沉船的挖掘得来。[27, 29]现代的越南青瓷是仿制品，产于Bat Trang窑，此窑是河内附近一直很受欢迎的著名遗址。已对样品进行了分析。[18]其他青瓷样品可以追溯到中国的南宋（1127-1279）和朝鲜半岛的高丽时期（918-1392）。

The last category of samples includes glazed *terra cottas* from different Islamic production centres, namely, Samarkand (Uzbekistan), Termez (Uzbekistan‐Afghanistan border), and Ifriqiya (Tunisia) (Figures 2 and 3).
最后一类样品是来自撒马尔罕（乌兹别克斯坦）、铁尔梅兹（乌兹别克斯坦-阿富汗边境）和Ifriqiya（突尼斯）等不同伊斯兰生产中心的釉陶（图2和3）。

They are mostly dated to the 14th century (Table 1). These samples have a different type of glaze composition from the porcelains and celadons with a considerable amount of PbO with a lower firing temperature (see previous studies [32,33] and references herein). The Afghan and Tunisian glazes are lead based whereas the Uzbek glaze is of the mixed lead‐alkaline type.
它们大多可以追溯到14世纪（表1）。这些样品含有大量氧化铅，不同于瓷器和青瓷的釉料成分，烧制温度较低（见先前的研究[32, 33]和本文的参考文献）。阿富汗和突尼斯的釉料是铅釉，而乌兹别克的釉料是铅碱混合釉。

2.2 | Methodological procedure |方法程序

Raman spectroscopy analyses on the glazes of the pottery samples were performed non‐invasively using a HR800 LabRam spectrometer (Horiba Scientific Jobin‐Yvon) coupled to a BX Olympus microscope equipped with different magnification objectives. Olympus ×100 ultralong working distance objective was used in order to be able to analyse the glaze layers more specifically in reproducible conditions whatever the shape of the pottery. The 457‐nm laser line generated by an Ar + ion laser (Coherent) source was mainly used for the collection of data with the illumination power on the samples of about 6 mW. The blue laser is very efficient in the analysis of glassy materials because it induces strong Raman scattering of the silicates. [34] The glaze layers of the samples were mostly analysed at two different points regardless of the colour. The maximum total counting time was 75 min, and the accumulations ranged from 3 to 50 to increase the signal‐to‐noise ratio. Each point was scanned in two different spectral windows, such as ~75‐2,355 cm −1 for the glass signature and ~2,110‐4,000 cm −1 for mainly the signature of the protonic species with 600 lines grating.
将HR800 LabRam光谱仪（Horiba Scientific Jobin‐Yvon）与具有不同放大倍率的物镜的BX Olympus显微镜连接，对陶瓷样品釉料进行非侵入性拉曼光谱分析。无论陶瓷形状如何，只要具备可复原的条件，使用Olympus×100超长工作距离物镜就能非常具体地分析釉层。主要靠氩离子激光（Coherent）源产生的457‐nm激光线采集数据，其在样品上的照明功率约为6 mW。蓝光对玻璃材料的分析是非常有效的，因为它能引起硅酸盐的强拉曼散射。[34] 无论颜色如何，只要有两个不同的点就可以分析大多数样品的釉层。最大总计数时间为75分钟，累计次数3到50次，以提高信噪比。每个点都由两个不同的光谱窗口进行扫描，例如玻璃信号为~75‐2355 cm −1，质子物质信号为

~2110 – 4000 cm −1，光栅为600线。

TABLE 1 The list of samples and their detailed description
表1样品列表及其详细描述

Label (Figure) 标签（图）	Type 类型	Date 日期	Origin 原产地	Remarks (largest dimension, cm) 备注（最大尺寸，cm）	Figures (Spectrum) 图（光谱）	References 参考文献
M-blb (lb) M-blb(lb)	Blue-and-white porcelain 青花瓷	Ming Dynasty (1368-1644) 明朝（1368-1644）	China 中国	Feldspar-based glaze (8.5) 长石釉（8.5）	8b-top 8b-上图	See similar artefacts in previous studies123251 |261 见先前研究中的类似手工艺品123251 | 261
M-blc (lc) M-blc(lc)	Blue-and-white porcelain 青花瓷	Ming Dynasty (1368-1644) 明朝（1368-1644）		Feldspar-based glaze (10) 长石釉（10）	8e-top 8e-上图	
Q-bl (lg) Q-bl(lg)	Wucai porcelain (blue underglaze; green, red overglaze) 五彩瓷器（釉下青花；绿色、红釉上彩）	Qing Dynasty (Kangxi reign, 1662-1722) 清朝（康熙年间，1662-1722）		Alkali-lime feldspar-based glaze with lead-based overglaze (5.5) 碱性石灰长石釉，铅基釉（5.5）	8f-top 8f-上图	
Q-r (If) Q-r(If)	Famille Rose porcelain (blue and green overglaze) 粉彩瓷器（蓝绿釉上彩）	Qing Dynasty (Yongzheng reign, 1723-1735) 清朝（雍正年间，1723-1735）		feldspar-based glaze with lead-based overglaze (9) 长石釉，铅基釉（9）	8a-top 8a-上图	
Q-p (le) Q-p(le)	Painted enamelled porcelain (blue, red, green, and yellow overglaze) 珐琅彩瓷（蓝、红、绿和黄釉上彩）	Qing Dynasty (Qianlong reign, 1736-1795) 清朝（乾隆年间，1736-1795）		Lead-based overglaze (9) 铅基釉（9）	8c-top 8c-上图	
F-p (la) F-p(la)	Blue-and-white porcelain 青花瓷	“Ming Dynasty” fake (21st century) “明代”仿制品（21世纪）		Feldspar-based glaze (6.5) 长石釉（6.5）	8d-top 8d-上图	
G-cel (3e) G-cel(3e)	Celadon 青瓷	Goryeo Dynasty (11th century) 高丽王朝（11世纪）	Korea 韩国	Lime glaze (10) 石灰釉（10）	7b-bottom 7b-下图	
Ly-cel 1 (3d) ly-cel 1（3d）	Celadon 青瓷	Ly Dynasty (12th-14th century) 李朝（12-14世纪）	Vietnam (Ha Lan kiln) 越南（Ha Lan窑）	Lime glaze (5) 石灰釉（5）	7f-bottom 7f-下图	[18,30] [18,30]
Ly-cel 2 (2d) ly-cel 2（2d）	Celadon 青瓷	Ly Dynasty (12th-13th century) 李朝（12-13世纪）		Lime glaze (10) 石灰釉（10）	7c-bottom 7c-下图	
Ly-bo (2c) Ly-bo(2c)	Stoneware 炻瓷	Ly Dynasty (12th century) 李朝（12世纪）		Lime glaze (6.5) 石灰釉（6.5）	7a-bottom 7a-下图	
S-cel (Id) S-cel(Id)	Celadon 青瓷	Southern Song (1127-1279) 南宋（1127-1279）	China 中国	Lime glaze (4) 石灰釉（4）	7e-bottom 7e-下图	See similar artefacts in Wood1311 见Wood1311中的类似手工艺品
F-cel (3f) F-cel(3f)	Celadon 青瓷	Fake (21st century) 仿制品（21世纪）	Vietnam (Bat Trang kiln) 越南（Bat Trang窑）	Lime glaze (5) 石灰釉（5）	7g-bottom 7g-下图	[181 [181
Ly-ti (2e) Ly-ti(2e)	Glazed tile or celadon 釉面瓦或青瓷	Ly Dynasty (13th century) 李朝（13世纪）	Vietnam 越南	Lime glaze (6.5) 石灰釉（6.5）	8b-bottom 8b-下图	
Le-bw (2a) Le-bw(2a)	Blue-and-white porcelain 青花瓷	Le Dynasty (15th century) 黎朝（15世纪）	Vietnam Cu Lao Cham 越南Cu Lao Cham	Feldspar-based glaze (3.5) 长石釉（3.5）	8a-bottom 8a-下图	[281 [281
Le-cel (2b) le-cel（2b）	Celadon 青瓷	Le Dynasty (15th century) 黎朝（15世纪）	shipwreck (Chit Dau kiln) 沉船（Chit Dau窑）	Lime glaze (5) 石灰釉（5）	8c-bottom 8c-下图	[27,29] [27,29]
Le-bwp (lh) Le-bwp（lh）	Blue-and-white porcelain bowl bottom 青花瓷碗底	Le Dynasty (15th century) 黎朝（15世纪）	Vietnam (Chit Dau kiln) 越南（Chit Dau窑）	Feldspar-based glaze (8.5) 长石釉（8.5）	8d-bottom 8d-下图	[271 [271
T-ti (2f) T-ti(2f)	Turquoise (blue) glazed terra cotta 青绿色（蓝色）釉陶	Timurid Dynasty (14th—15th century) 帖木儿王朝（14—15世纪）	Uzbekistan (Samarkand) 乌兹别克斯坦（撒马尔罕）	Lead-alkaline glaze (9) 铅碱釉（9）	7c-top 7c-上图	
T-p (3a) T-p(3a)	Yellow glazed terra cotta 黄色釉陶	(14th century) （14世纪）	Afghanistan border (Termez) 阿富汗边境（铁尔梅兹）	Lead-based glaze (7) 铅釉（7）	7a-top 7a-上图	[321 [321
T-b (3b) T-b(3b)	Blue glazed terra cotta 蓝色釉陶	(14th century) （14世纪）	Tunisia (Ifriqiya) 突尼斯（Ifriqiya）	Lead-based glaze (10) 铅釉（10）	7d-top 7d-上图	[331 [331
T-bb (3c) T-bb(3c)	Blue and brown glazed terra cotta 蓝色和棕色釉陶	(14th century) （14世纪）		Lead-based glaze (6) 铅釉（6）	7b-top 7b-上图	[331 [331

TABLE 2 The list of reference stained glass samples with artificial corrosion and their detailed description
表2经人工腐蚀的参考彩色玻璃样品的列表及其详细说明

Label 标签	Type (colour) 类型（颜色）	Date (century) 年代（世纪）	Origin 原产地	Remarks 备注
LM13b - 2 LM13b - 2	K - Ca glass (blue) 钾钙玻璃（蓝色）	13th 13世纪	Le Mans cathedral 勒芒大教堂	
LM13 - 15b - 1 LM13 - 15b - 1	K - Ca glass (blue) 钾钙玻璃（蓝色）	ca. 13th to 15th 约13-15世纪		Annealed at 600 °C 在600℃下退火
AM19b - 1 AM19b - 2 AM19b - 1 AM19b - 2	Na - Ca glass (blue) 钠钙玻璃（蓝色）	19th 19th 19世纪 19世纪	Amiens cathedral 亚眠大教堂	K^+ ion exchanged k +离子交换
AM13y AM13y	K - Ca glass (yellow) 钾钙玻璃（黄色）	13th 13世纪		



FIGURE 1 Chinese (a: F - p; b: M - blb; c: M - blc; d: S - cel; e: Q - p; f: Q - r; g: Q - bl) and Vietnamese (h: Lê - bwp) porcelains and celadon (see Table 1 for details) [Colour figure can be viewed at wileyonlinelibrary.com]
图1中国(a:F - p; b:M - blb; c:M - blc; d:S - cel; e:Q - p; f:Q - r; g:Q - bl)和越南(h:Lê - bwp)的瓷器和青瓷（详见表1）[彩图请浏览wileyonlinelibrary.com]

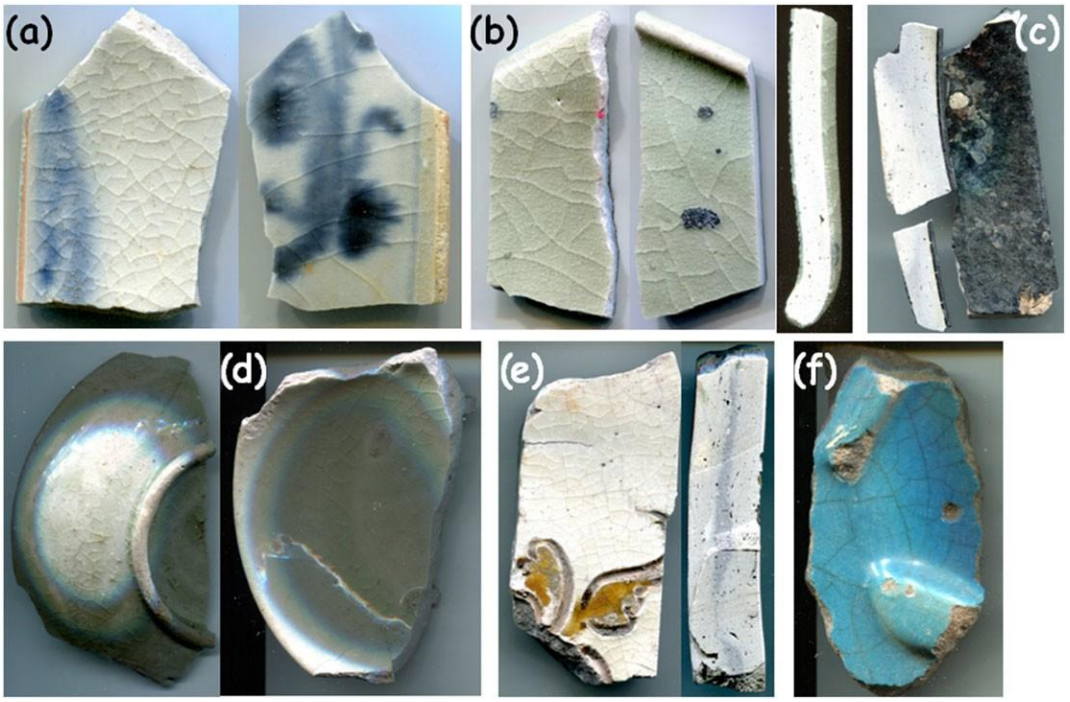


FIGURE 2 Vietnamese pottery (a: Lê ‐ bw; b: Lê ‐ cel; c: Ly ‐ Bo; d: Ly ‐ cel 2; e: Ly ‐ ti) and glazed *terra cotta* from Samarkand (f: T ‐ ti; see Table 1 for details) [Colour figure can be viewed at wileyonlinelibrary.com]

图2越南陶器(a:Lê ‐ bw; b:Lê ‐ cel; c:Ly ‐ Bo; d:Ly ‐ cel 2; e:Ly ‐ ti)和撒马尔罕的釉陶（f:T ‐ ti；详见表1）[彩图请浏览wileyonlinelibrary.com]

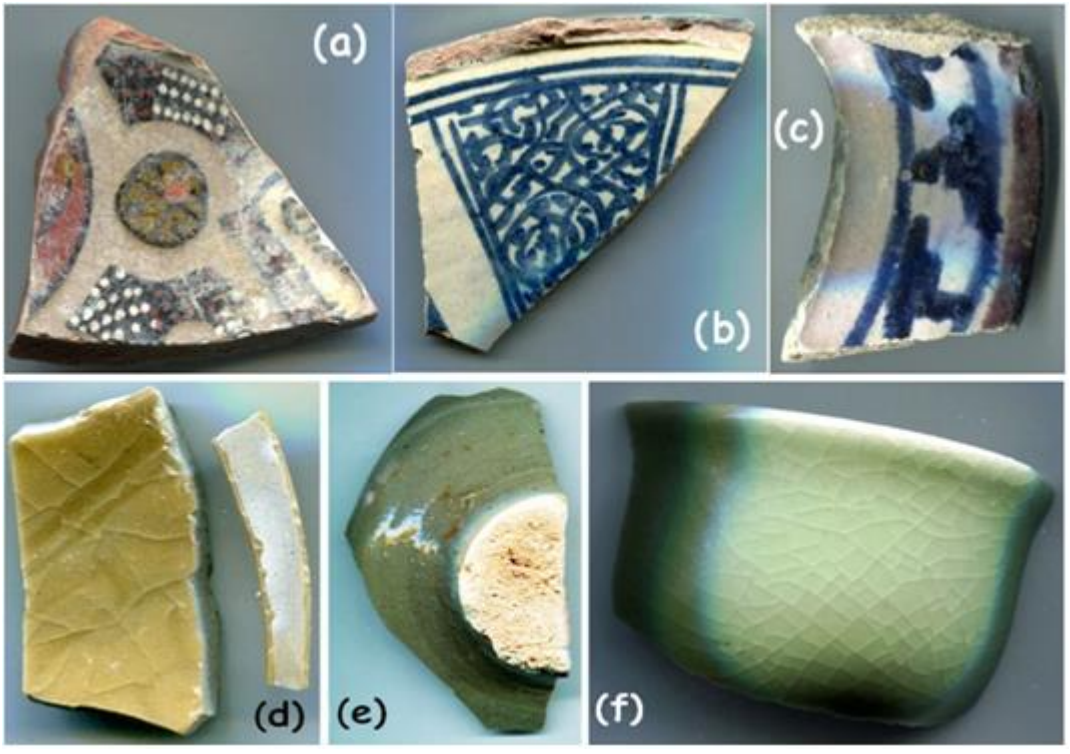


FIGURE 3 Glazed *terra cottas* from Termez (a: T ‐ p) and Ifriqiya (b: T ‐ b; c: T ‐ bb), Vietnamese (d: Ly ‐ cel 1; f: F ‐ cel), and Korean (e: G ‐ cel) celadons (see Table 1 for details) [Colour figure can be viewed at wileyonlinelibrary.com]

图3铁尔梅兹(a:T ‐ p)和Ifiqiya(b:T ‐ b; c:T ‐ bb)的釉陶；越南(d:Ly ‐ cel 1; f:F ‐ cel)和朝鲜(e:G ‐ cel)的青瓷（详见表1）[彩图请浏览wileyonlinelibrary.com]

This grating provides a large spectral window that allows collecting the 2,110–4,000 cm^{-1} range in one shot without the need to combine the spectra as required in the case of using a grating with a high line number.

该光栅有一个大光谱窗口，可以一次采集2,110–4,000 cm^{-1}的范围，而且不需要在使用高线数光栅的情况下组合所需光谱。

This is very important because it allows the analysis of broad tiny bands.

这一点非常重要，因为它可以分析各种各样的微小谱带。

The vibrational modes including the protons are expected in the wavenumber region between 2,000 and 3,800 cm^{-1} (the narrow Raman signature of isolated vibrators such as hydroxyl groups being expected in the 3,500–3,800 cm^{-1} range although those of more or less strongly hydrogen‐bonded species between 2,000 and 3,200 cm^{-1}). [8,9,11,20,35–38] Each spectrum obtained in the high wavenumber region was mathematically corrected by using LabSpec 5 software according to the procedure recommended by the instrument supplier for the elimination of the interference waves arising from the notch filter, which become visible when the scattered intensity is very low.

质子在振动模式下的波数范围预计可以达到2,000至3,800 cm^{-1}（虽然或多或少有些强氢键物质的拉曼信号在2,000至3,200 cm^{-1}之间，但独立的原子团如羟基等的窄拉曼信号预计可以达到3,500至3,800 cm^{-1}）。[8, 9, 11, 20, 35–38] 使用LabSpec 5软件，按照仪器供应商建议的程序对在高波数区域获得的各光谱进行数学校正，当散射强度非常低时，可以看到由陷波滤波器产生的干扰波，然后进行消除。

The experimental procedure was extended with the use of a higher magnification objective (×200 Mitutoyo), a smaller (100 μm) confocal hole, and a different laser wavelength (514 nm) in order to compare the quality of the spectra obtained. Our experience in the study of aluminosilicates [34,39] and protonic species [11,20] convinces us that blue or violet laser lines are the most efficient for the study of silicates (and of protonic species) due to the factors such as the combination of ν^4 dependence of Raman scattering, [19] good efficiency of mirrors and charge‐coupled device (CCD) detector, high‐laser intensity, and preresonance of Si–O bond. For the purpose of comparison, representative samples that display a good signal of the protonic species were selected for each step. A very high magnification (×200) objective allows the analysis of the very surface and probes a volume of approximately 0.5 × 0.5 × 2 μm^3 to be compared with that of 2 × 2 × 6 μm^3 for ×100 objective (measurement based on the procedure reported in Havel and Colomban [40]). Very high magnification objective gives a very good spectrum by focusing on a single phase, a fluorescence‐free grain but requires a more sensitive focus adjustment on the sample by checking the Raman signal while moving the objective at the same time. In this case, the total counting time was usually increased by a factor of 3. The 514‐nm laser line was also produced by the Ar^+ ion laser source with an average illumination power of ~10 mW on the samples.

为了比较所获得光谱的质量，使用了较高倍物镜（×200 Mitutoyo）、更小的（100μm）共焦孔和不同波长（514 nm）的激光来扩展实验程序。我们在研究铝硅酸盐[34, 39]和质子物质[11, 20]方面的经验使我们相信，蓝色或紫色激光线对于硅酸盐（和质子物质）的研究是最有效的，这得益于拉曼散射ν^4依赖性的组合、[19]反射镜和电荷耦合器件（CCD）探测器的良好效率、高激光强度和硅氧键的预共振等因素。出于比较的目的，每个步骤都选择了显示质子物质良好信号的代表性样品。超高倍（×200）物镜适用于最表层分析，可以探测到大约0.5×0.5×2 μm^3的体积，相比之下，×100物镜可以探测到的体积为2×2×6 μm^3（按照Havel和Colomban报告中的程序进行的测量[40]）。将超高倍物镜聚焦在单相无荧光纹理上，可以得到非常好的光谱，但是需要在移动物镜的同时检查拉曼信号，更精准地调整对样品的聚焦。在这种情况下，总计数时间通常增加3倍。514‐nm激光线由氩离子激光源产生，样品的平均照明功率约为10 mW。

3 | RESULTS
|结果

3.1 | Reference corroded glass samples
|参考腐蚀玻璃样品

The wave‐corrected Raman spectra for the reference stained glass samples previously studied [8] are given in Figure 4. Raman analyses of these samples with different chemical compositions gave variable signatures between 2,100 and 4,000 cm^{-1}, assigned to the protonic species at the surface layer of the glass network (Tables 2 and 3). Here, the glasses analysed belong to two types, such as potash‐lime glass (sensitive to water corrosion) and soda‐lime glass (relatively more stable against corrosion). Figure 4b shows the spectrum of a corroded blue potash‐lime type of glass (LM13‐15b‐1) with a notable Raman signature of protonic species.

先前研究的参考彩色玻璃样品[8]的波修正拉曼光谱如图4所示。对具有不同化学成分的这些样品进行拉曼分析，得出玻璃网络表层的质子物质的各种信号范围在2100至4000 cm^{-1}之间（表2和表3）。本文分析的玻璃分为两种类型：钾钙玻璃（对水腐蚀敏感）和碱石灰玻璃（抗腐蚀性相对更稳定）。图4b是受腐蚀的蓝色碱石灰玻璃（LM13‐15b‐1）的光谱，其质子物质的拉曼信号非常强。

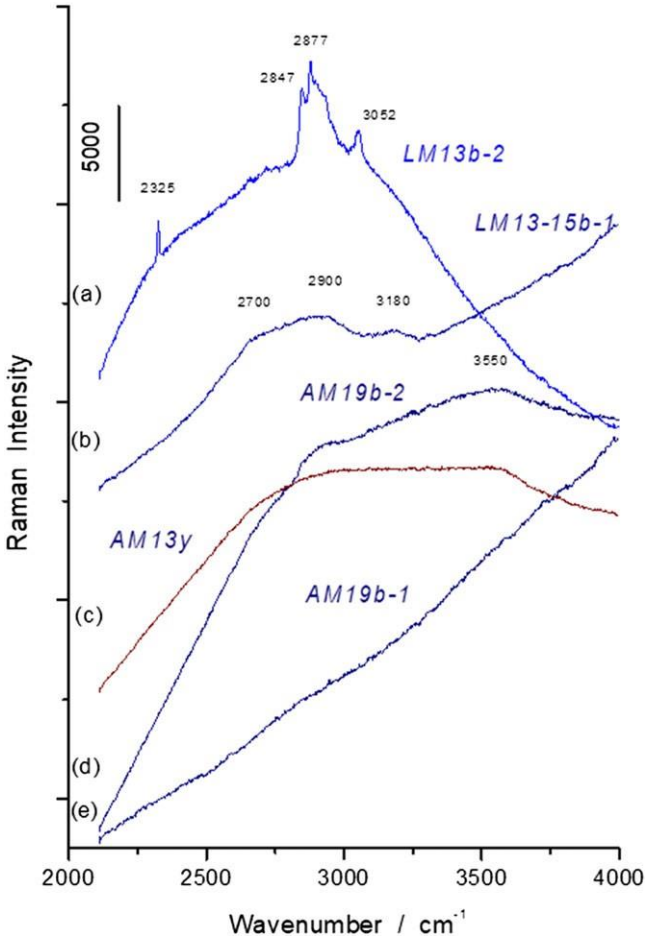


FIGURE 4 Representative wave‐corrected Raman spectra recorded on artificially corroded stained glass pieces: lime‐potash medieval (LM13b‐2, LM13‐15b‐1, and AM13y) and soda‐lime 19th century glasses (AM19b‐1, AM19b‐2; ×100 objective; confocal hole: 200 μm; see Table 2 for more details) [Colour figure can be viewed at wileyonlinelibrary.com]

图4人工腐蚀彩色玻璃片的代表性波修正拉曼光谱：中世纪钾钙玻璃(LM13b‐2、LM13‐15b‐1、AM13y)和19世纪碱石灰玻璃（AM19b‐1、AM19b‐2；×100物镜；共焦孔：200μm；详见表2）[彩图请浏览wileyonlinelibrary.com]

This sample had been annealed in air at 600 °C after the corrosion process in boiling H_2SO_4 and then exposed to air. [8] This process actually cleans the very surface of glass and eliminates the poorly H‐bonded species. A broad component is observed with submaxima at 2,700, 2,900, and 3,180 cm −1. The broad bands at 2,700 and 2,900 cm^{-1} indicate the strongly H‐bonded species whereas the band at 3,180 cm^{-1} is assigned to the water molecules adsorbed at the glass surface or within the cracks. [8,16] A weak broad band visible at 3,300 cm^{-1} also indicates the presence of water molecules in the sample whereas another weak narrow band at 3,730 cm^{-1} is assigned to the hydroxyl groups (Table 3 and Figure 4b). The spectra of a yellow potash‐lime glass (AM13y; Figure 4c) and a blue soda‐lime glass (AM19b‐2; Figure 4d) also display somewhat similar Raman signatures of protonic species with weaker intensity.

样品在沸腾的H_2SO_4中腐蚀后，在600℃的空气中退火，然后暴露于空气中。[8]这个过程实际上清洁了玻璃表面，消除了氢键结合不良的物质。在2700、2900、 和3180 cm^{-1}处观察到仅次于最大值的宽谱分量。2700和2900 cm^{-1}处的宽谱带表示强氢键物质，而3180 cm^{-1}处的谱带表示吸附在玻璃表面或裂纹内的水分子。[8, 16]在3300 cm^{-1}处可见的弱宽谱带同样表明样品中存在水分子，而在3730 cm^{-1}处的另一个弱窄谱带表示羟基（表3和图4b）。黄色钾钙玻璃（AM13y；图4c）和蓝色碱石灰玻璃（AM19b‐2；图4d）也显示了类似的拉曼信号，表示质子物质的强度较弱。

TABLE 3 The observed Raman band wavenumbers and bandwidths of the samples and their assignments
表3样品的拉曼谱带波数和带宽及其代表物质

Wavenumber (cm^{-1}) **波数(cm^{-1})**	**Bandwidth** **带宽**	**Materials** **材料**	**Assignment** **指示**	**Corresponding IR band wavenumbers (cm^{-1})** [8,20,21] 相应的红外谱带波数（cm^{-1}）[8，20，21]
3,750	vb	Porcelain	Hydroxyl groups	3,600–3,800
3,750	vb	陶瓷	羟基	3,600-3,800
3,730	n	*Stained glass*		
3,730	n	*彩色玻璃*		
		Glazed *terra cotta*		
		釉陶		
		Celadon or stoneware		
		青瓷或炻瓷		
3,560	n	Porcelain overglaze		
3,560	n	瓷釉		
3,550	vb	Stained glass		
3,550	vb	彩色玻璃		
		Glazed *terra cotta*		
		釉陶		
3,510	n	Glazed *terra cotta*		
3,510	n	釉陶		
3,300	n	Stained glass	Water	3,200–3,500
3,300	n	彩色玻璃	水	3,200-3,500
		Celadon or stoneware		
		青瓷或炻瓷		
3,230	b	Porcelain (shipwreck)		
3,230	b	瓷器（沉船）		
3,180	vb	Stained glass		
3,180	vb	彩色玻璃		
		Porcelain overglaze		
		瓷釉		
3,170	vb	Celadon or stoneware		
3,170	vb	青瓷或炻瓷		
2,950	vb	Glazed *terra cotta*	H‐bonded species	2,500–3,500
2,950	vb	釉陶	氢键物质	2,500-3,500
		Celadon or stoneware		
		青瓷或炻瓷		
2,940	b	Porcelain (shipwreck)		
2,940	b	瓷器（沉船）		
2,920	b	Porcelain overglaze		
2,920	b	瓷釉		
2,900	vb	Stained glass		
2,900	vb	彩色玻璃		
		Porcelain overglaze		
		瓷釉		
2,850	n	Porcelain		
2,850	n	陶瓷		
2,750	vb	Glazed *terra cotta*		
2,750	vb	釉陶		
2,700	vb	Stained glass		
2,700	vb	彩色玻璃		
		Glazed *terra cotta*		
		釉陶		
		Celadon or stoneware		
		青瓷或炻瓷		
		Porcelain overglaze or (shipwreck)		
		瓷釉或（沉船）		

Note. n: narrow; b: broad; vb: very broad.
注：n：窄；b：宽；vb：极宽。

These glass pieces conserved in ambient air after the corrosion process (and washing) [8] show an additional feature at ~3,550 cm^{-1}, according to the poorly H‐bonded protonic species (Tables 2 and 3). The spectrum of sample LM13b‐2 (Figure 4a), a blue potash‐lime glass that was inserted in KNO_3 to exchange protonic species with K^+ ions shows narrower peaks at 2,847, 2,877, and 3,052 cm^{-1} characteristic of trapped organic molecules within the cracks (samples have been washed with water and ethanol). Their signature is very different from that of protonic species in terms of wavenumber and bandwidth. The very narrow peak at around 2,325 cm^{-1} is due to the signature of N_2 gas [41] trapped from the air in bubbles during the production of glass. Its observation is common in glass, glaze, and ceramic body as that of O_2 at 1,555 cm^{-1} because the multireflection of the light at the bubble‐matrix interface increases the Raman intensity. The last spectrum corresponds to a blue soda‐lime glass (AM19b‐1) with no visible signature of protonic species (Figure 4e).

This is most probably due to the composition of the sample because soda‐lime glasses are more corrosion resistant than the potash‐lime ones.[8,22]

氢键结合不良质子物质（表2和表3）腐蚀（和清洗）后保存在环境空气中的玻璃碎片[8]在~3550 cm^{-1}处显示出额外的特征。样品LM13b‐2（图4a）是一种蓝色钾钙玻璃，将其插入硝酸钾中，与钾离子交换质子物质后，其光谱显示2847、2877和3052 cm^{-1}处有较窄峰，表示裂缝中截留的有机分子（样品用水和乙醇洗涤）。就波数和带宽而言，它们的信号与质子物质非常不同。在大约2325 cm^{-1}处出现非常窄的峰是由于玻璃中有氮气气泡[41]，该气泡在玻璃生产过程中形成。玻璃、釉料和陶瓷体中的氮气观察值与氧气在1555 cm^{-1}时的观察值相同，因为光在气泡基质界面的多次反射增加了拉曼强度。最后一个光谱对应的是蓝色碱石灰玻璃（AM19b‐1），未看见质子物质的信号（图4e）。这很可能是因为样品的成分引起，因为碱石灰玻璃比钾钙玻璃更耐腐蚀。[8,22]

The analyses of these glasses by IR absorption on thick samples give rise to strong absorption in the same wavenumber range but also in the nIR region (combinations and overtones), and their assignment is well documented (see previous studies [8,21] and references herein). This confirms that Raman microspectrometry allows detecting the signature of the protonic species present in the very surface of glass, although its sensitivity is less than those of IR and nIR absorption.

对这些玻璃的厚样品进行红外吸收分析，在相同的波数范围和近红外区（合谱和泛频峰）都产生了强吸收。这些信号都有相关记录（见先前的研究[8, 21]和本文的参考文献）。这证实显微拉曼光谱技术能够检测玻璃表面质子物质的信号，尽管其灵敏度低于红外和近红外吸收。

3.2 | Choice of the “best” experimental parameters

|选择“最佳”实验参数

Raman spectra were compared by using 514‐nm laser wavelength, ×200 objective, and 100‐μm confocal hole on the same samples for each experimental step. The analyses with the green laser were performed on samples Q‐r and T‐p that show stronger signatures of the protonic species with the blue laser (Table 3). The spectra obtained show very weak signature of the protonic species but some additional cosmic peaks recognized by the one pixel‐width (Figures 5a and S1). The results confirmed that blue laser is the most efficient one for detecting the protonic species. For the objective comparison, sample M‐blb was selected due to its strong signal of the protonic species in the glass network (Figure 5b, A–A′; Table 3).

要比较拉曼光谱，须在每个实验步骤中，对相同的样品使用514-nm激光波长、×200物镜和100μm共焦孔。对在蓝色激光下显示出较强质子物质信号的样品Q‐r和T‐p，使用绿色激光进行分析（表3）。所获得的光谱显示质子物质的信号非常微弱，但是一些额外的宇宙峰可用一个像素宽度识别（图5a和S1）。结果证实，蓝色激光是探测质子物质最有效的方法。为了进行客观比较，选择了在玻璃网络中质子物质信号较强的样品M‐blb（图5b，A–A′；表3）。

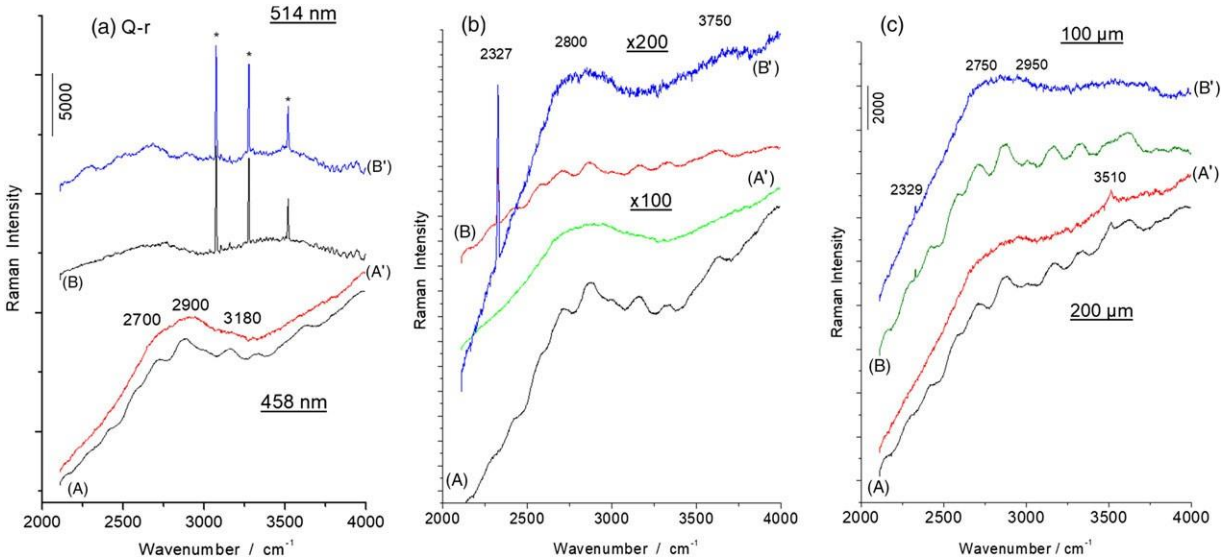


FIGURE 5 Comparison of Raman spectra recorded on the same sample with different experimental parameters: (A,B) as recorded; (A′,B′) spectra after subtraction of the waves due to the filtering. (a) Spectra of Q‐r obtained with green (10 mW at the sample) and blue (6 mW at the sample) lasers; (b) Spectra of M‐blb obtained with ×200 and ×100 microscope objectives; (c) Spectra of T‐p obtained with 100 and 200 µm confocal hole (*: Cosmic peak, see text for more details) [Colour figure can be viewed at wileyonlinelibrary.com]

图5同一样品不同实验参数的拉曼光谱比较：(A,B)为记录参数；(A′,B′)为滤波后得到的滤波光谱。(a)使用绿色激光（样品照明功率10 mW）和蓝色激光（样品照明功率6 mW）获得的Q‐r光谱；(b)使用×200和×100显微镜物镜获得的M‐blb光谱；(c)使用100µm和200µm共焦孔获得的T‐p光谱（*：宇宙峰的详细定义见描述）[彩图请浏览wileyonlinelibrary.com]

Raman analysis of the same sample with ×200 objective allowed us to obtain a better signal with higher intensity with an apparent feature at 3,750 cm −1, which is assigned to the hydroxyl groups (Figure 5b, B–B′; Table 3). However, the recording time was increased about three times together with the decrease of the signal-to-noise ratio because the laser spot was much smaller. Here, it should be noted that it is impossible to analyse the same point with different high magnification objectives and the OH − groups are probably distributed heterogeneously. For the confocal hole comparison, analyses were performed on sample T-p also showing a strong signal with the standard parameters (Figure 5c, A–A′; Table 3). The intensity of the Raman signal was also increased with the use of a smaller confocal hole, but the OH − peak at 3,510 cm −1 was no longer visible, perhaps due to some local heating that eliminated the poorly H- bonded species at the very surface (Figure 5c, B–B′).

使用×200物镜对同一样品进行拉曼分析能够获得更好、更高强度的信号，在3750 cm −1处具有明显的特征，代表羟基（图5b，B–B′；表3）。然而，由于激光光斑小得多，记录时间增加了大约三倍，同时信噪比也有所降低。这里，应该注意的是，不可能用不同的高倍物镜分析同一个点，而且羟基可能是不均匀分布。为了进行共焦孔对比，样品T-p的分析也显示了具有标准参数的强烈信号（图5c，A–A′；表3）。使用更小的共焦孔，拉曼信号的强度也相应增加，但是在3,510cm-1处的羟基峰值不再可见，这也许是由于局部加热消除了最表层的氢键结合不良的物质（图5c，B–B′）。

3.3 | The glaze signature

|釉料信号

The silicate glasses may comprise a wide range of compositions based on the different types of their raw materials that are mainly the fluxes such as potash, soda, lime, and lead. In the history of glazed pottery, different types of glass compositions had been used in the preparation of the glazes according to the availability of raw materials, technical competence of the period (kiln maximal temperature), and experimentations of the craftsmen. [24,31]

根据不同类型的原材料，硅酸盐玻璃可能包含多种成分，这些原材料主要是熔剂，例如碳酸钾、苏打、石灰和铅。在釉陶的发展史中，依据原料的实用性、当时的技术能力（窑最高温度）和工匠的经验，在釉料的制备过程中使用了不同类型的玻璃成分。[24,31]

All types of glassy silicates give a characteristic Raman spectrum, which mainly consists of two broad bands found at ~500 and ~1,000 cm $^{-1}$. These are the Si–O bending and stretching modes respectively, which display the fundamental vibrational modes of the SiO_4 tetrahedral units making up the glass network. [34,42–44] The incorporation of different types of fluxes in the silicate structure has a direct effect on the Raman signature in terms of the spectral position of the bands and their relative intensities. Thus, the evaluation of these parameters in the Raman spectra enables us to identify different composition types. [34,39,42–46] The different components of the Si– O stretching bands arise from the different population of the SiO_4 tetrahedra in the form of isolated and more or less connected arrangements. It has been pointed out both experimentally [45,46] and by modelling [47] that the area ratio of bending to stretching band is directly related to the degree of polymerization of the SiO_4 vibrational (and chemical) unit and hence to the melting temperature of glass.

所有类型的玻璃硅酸盐都有特定的拉曼光谱，它主要由在约500和约1000cm^{-1}处发现的两个宽谱带组成。这些分别是硅氧弯曲和伸缩模式，它们显示了构成玻璃网络的SiO_4四面体单元的基本振动模式。[34, 42–44]硅酸盐结构中结合不同类型的熔剂对拉曼信号有直接影响，具体表现在谱带的光谱位置及其相对强度上。因此，拉曼光谱中这些参数的评估使我们能够识别不同的组成类型。[34, 39, 42–46]硅氧伸缩谱带的不同成分来自不同群体的SiO_4四面体，其形式为孤立的或多或少相连的排列。通过实验[45, 46]和建模[47]可知，弯曲与伸缩谱带的面积比与SiO_4振动（和化学）单元的聚合度直接相关，因此与玻璃的熔化温度直接相关。

The representative Raman spectra obtained from the glazes of the pottery samples are given in Figure 6. All spectra display the characteristic Raman signature of a silicate type of glass: two broad features at about 450 and 1,000 cm $^{-1}$, which represent the Si–O bending and stretching modes, respectively. [45–47] For the porcelain glazes with silica‐rich composition that have a high melting temperature (approximately 1350–1400 °C), the bending mode band is much stronger than the stretching one (Figure 6a,b,d,e). [46] An opposite behaviour is observed for low temperature melting lead‐rich glazes (approximately 700–800 °C) such as in the cases of Islamic *terra cotta* glaze (Figure 6f) and the overglaze of Chinese Qing porcelain sample (Figure 6h).

从陶器样品釉料中获取的具有代表性拉曼光谱如图6所示。所有光谱都显示了硅酸盐玻璃的拉曼信号特征：在大约450和1000cm^{-1}处的两个宽谱带特征，分别代表硅氧弯曲和伸缩模式。[45–47]对于具有高熔点（约1350–1400℃）的富含二氧化硅成分的瓷釉，弯曲模式谱带比伸缩模式谱带强得多（图6a、6b、d、e）。[46]在低熔点富铅釉（约700-800℃）中，例如伊斯兰釉陶（图6f）和中国清代陶瓷样品的釉上彩（图6h），却观察到相反的行为。

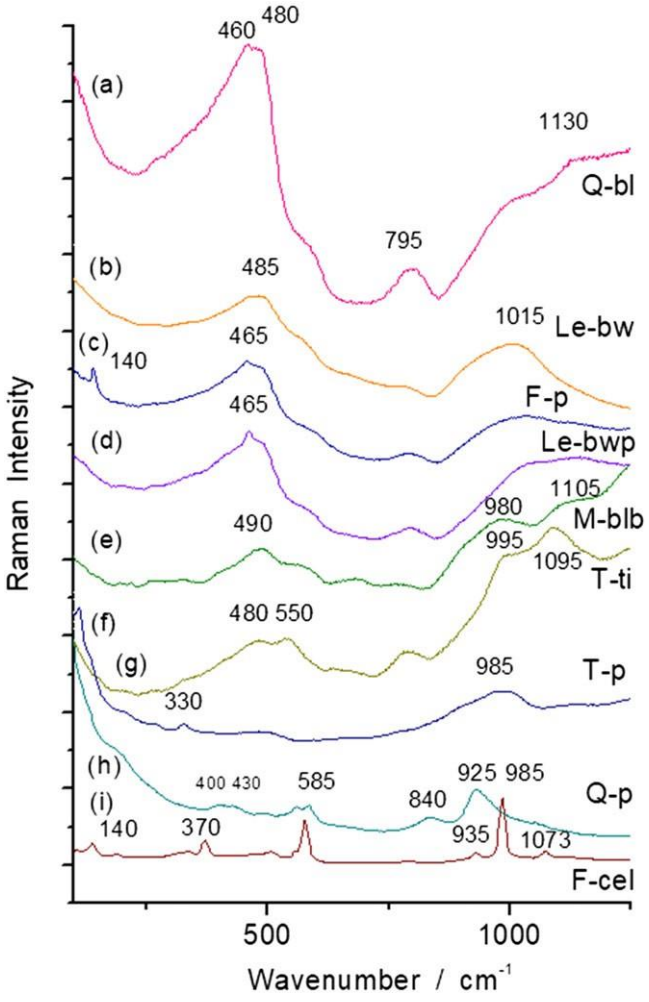


FIGURE 6 Representative Raman spectra of the different types of glazes collected from different coloured areas of the samples (×100 objective; c.h.: 200 μm): (a) Q-bl white, (b) Lê-bw blue, (c) F-p white, (d) Lê-bwp white, (e) M-blb blue, (f) T-p yellow, (g)T-ti turquoise, (h) Q-p green, and (i) F-cel green (see also Table 1 for more details) [Colour figure can be viewed at wileyonlinelibrary. com]
图6从样品的不同颜色区域收集的不同类型釉料的代表性拉曼光谱（×100物镜；c. h.：200μm）：（a）Q-bl白色，（b）Lê-bw蓝色，（c）F-p白色，（d）Lê-bwp白色，（e）M-blb蓝色，（f）T-p黄色，（g）T-ti蓝绿色，（h）Q-p绿色，和（I）F-cel绿色（详见表1）[彩图请浏览wileyonlinelibrary. com]

Several narrow peaks (quartz at 465 cm −1, α-wollastonite at 585 and 985 cm −1) are also observed in some of the glaze spectra arising from the crystalline precipitates within the glaze. [34,46] The durability of the glaze is directly related to its chemical composition as in the case of feldspar-based porcelain glazes where the addition of aluminium increases the chemical stability. [48] On the contrary, lead-rich glass can easily be corroded by water. [48,49]

从釉料的结晶沉淀物中也观察到一些釉谱有几个窄峰（石英：465cm-1处；α-硅灰石：585和985cm-1处）。[34，46]釉料的耐久性与其化学成分直接相关，例如长石基瓷釉，可以通过添加铝提高化学稳定性。[48]相反，富铅玻璃很容易被水腐蚀。[48,49]

We will first discuss the data regarding the lead- glazed terra cottas (the a priori more reactive glaze with low polymerization index), then those of celadons or stoneware (firing at higher but medium temperature) and porcelains in which the glaze is fired at high temperature and has the maximal index of polymerization, that is, the less number of exchangeable cations.
我们将首先讨论铅釉陶（聚合指数较低的先天活性釉）的数据，然后讨论青瓷或炻瓷（在较高但中等温度下烧制）和在高温下烧制且聚合指数最大的瓷釉的数据，即可交换阳离子的数量较少。

3.4 | Glazed *terra cottas* |釉陶

The wave-corrected Raman spectra for the glazed terra cottas are given in Figure 7 on the left. The Raman signal of the protonic species is rather strong since these glazes have a high reactivity due to the lead-based composition. In particular, the yellow-coloured glaze of the sample from Termez (T-p) displays a strong signal with the broad features at 2,700 and 2,950 cm −1 (Table 3; Figure 7a, left). Here, it should be noted that the yellow pigments used are rich in lead, which is a factor also contributing to the corrosion process. [48–50] The “narrow” peak at 3,510 cm −1 that is assigned to the hydroxyl groups is also significant (and seems associated to the lead-based glaze, see further). Another small band at 3,730 cm −1 also indicates the presence of hydroxyl groups. The spectra of other glazed terra cottas also show rather similar features of the protonic species but with variable intensities (Figure 7b,c,d, left). In fact, the white glaze of the Tunisian sample (T-bb) displays the least marked signal among the others. Additionally, the blue glaze of the sample from Tunisia (T-b) displays an apparent very broad band at 3,550 cm −1 rising from the OH − groups as well as the N 2 gas peak at 2,325 cm −1 (Table 3). Please note that all of the samples are dated to the same time period.

图7左侧是釉陶的波修正拉曼光谱。因为这些釉料基于铅成分具有高反应性，质子物质的拉曼信号相当强。特别是，Termez（T-p）样品的黄色釉料在2700和2950 cm-1处显示出强烈的信号，具有宽谱带特征（表3；图7a，左图）。这里，要注意的是所用的黄色颜料富含铅，这也是加速腐蚀的一个因素。[48–50]表示存在羟基的3,510cm-1处的“窄”峰也很明显（似乎与铅基釉料有关，详见下文）。3,730cm-1处的另一个小谱带也表明存在羟基。其他釉陶的光谱也显示出质子物质相当相似的特征，但强度不同（图7b，c，d，左图）。事实上，突尼斯样品（T-bb）的白色釉料显示的信号最不明显。此外，突尼斯样品的蓝色釉料在3550cm-1处显示出明显的极宽谱带，表明存在羟基，也在2,325cm-1处也显示有N 2气体峰 （表3）。请注意，所有样品的日期都是同一时期。

3.5 | Glazed celadons or stoneware |釉青瓷或炻瓷

Figure 7, right compares the wave-corrected spectra obtained from the celadons or stoneware that have a lime-based composition. The stoneware sample (Ly-bo) that is one of the oldest samples from the 12th century shows a very strong Raman signal of the protonic species (Figure 7a, right). The broad features at 2,700 and 2,950 cm −1 are again visible, displaying the H-bonded species found in the glass network. Additional features at 3,170 and 3,300 cm −1 are also present, which are assigned to the water molecules adsorbed on the surface.

图7右图比较了青瓷或有石灰基成分的炻瓷的波修正拉曼光谱。炻瓷样品（Ly-bo）是12世纪以来最古老的样品之一，显示出质子物质非常强的拉曼信号（图7a，右图）。在2700和2950cm-1处的宽谱带特征再次可见，表示存在在玻璃网络中发现的氢键物质。在3170和3300cm-1处也有附加特征，这些特征表示存在吸附在表面上的水分子。

Another feature at 3,730 cm −1 is assigned to the hydroxyl groups (Table 3). The spectrum of the 11th century Korean sample (G-cel) is also consistent with that of the stoneware sample, showing a similar but less intense signature (Figure 7b, right). The spectrum of the Vietnamese sample (Ly-cel 2) shows a rather similar spectrum with lower intensity (Figure 7c, right) whereas spectra of the other ancient celadons represent rather different signatures with varying intensities (Figure 7d,e,f, right).

在3730cm-1处的另一个特征表示存在羟基（表3）。11世纪韩国样品的光谱也与炻瓷样品一致，显示出相似但不太强烈的特征（图7b，右图）。越南样品的光谱（Ly-cel 2）显示了强度较低而且相当相似的光谱（图7c，右图），而其他古代青瓷的光谱代表了强度不同也相当不同的特征（图7d，e，f，右图）。

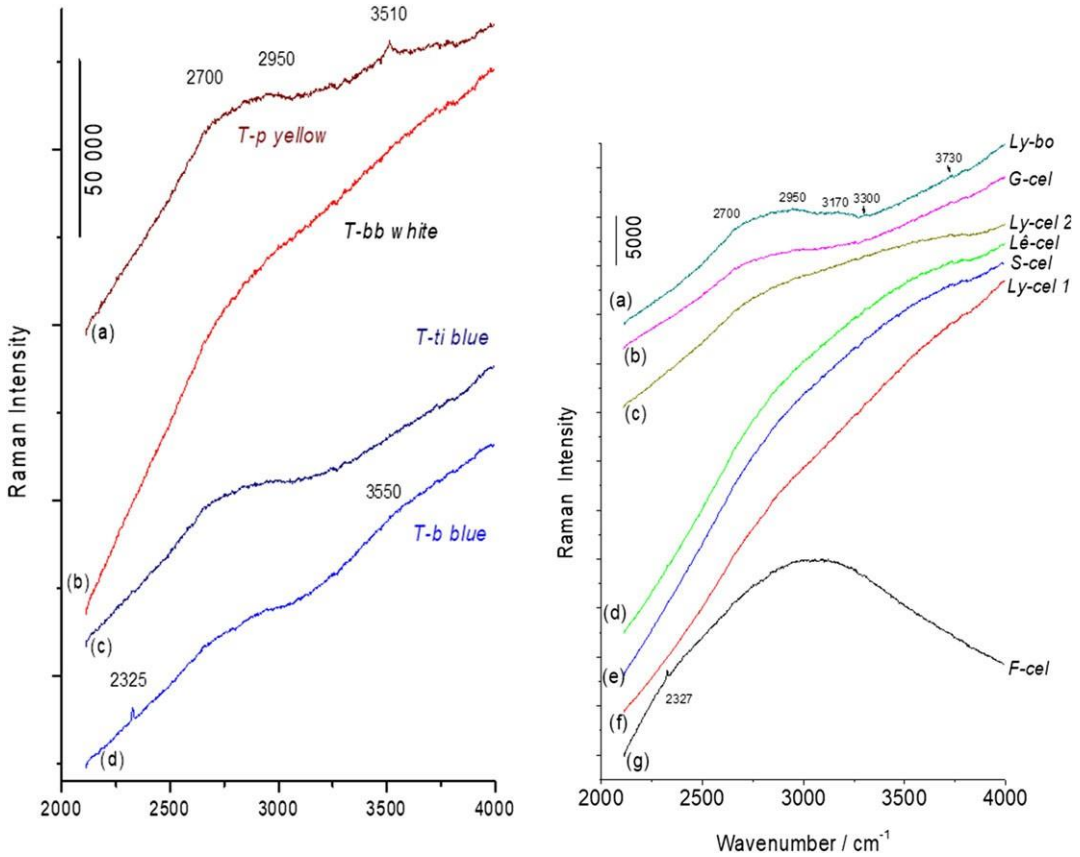


FIGURE 7 Representative wave‐corrected Raman spectra recorded on glazed *terra cottas* (left) and celadons or stoneware (right; ×100 objective; c.h.: 200 μm; see Table 1 for more details) [Colour figure can be viewed at wileyonlinelibrary.com]
图7釉陶（左图）和青瓷或炻瓷（右图）的代表性波修正拉曼光谱；×100物镜；c.h.: 200μm；详情见表1） [彩图请浏览wileyonlinelibrary.com]

After all, the modern celadon sample (F-cel) displays a completely different type of spectrum where actually no signature of the protonic species is visible (Figure 7g, right). The big bump peaking at ~3,000 cm −1 is characteristic of fluorescence. The peak at 2,327 cm −1 is again assigned to N 2 gas. Thus, Raman signatures of the protonic species obtained in the celadons or stoneware seem to be in correlation with their ages, but other factors should also be considered such as the mechanical damage (cracks, voids) as a function of the degree of corrosion.

毕竟，现代青瓷样品(F-cel)显示了一种完全不同类型的光谱，它看不到质子物质的特征（图7g，右图）。荧光的特征是顶峰值约在3,000cm-1处。在2327cm-1处的峰值再次表示存在N 2气体。因此，在青瓷或炻瓷中获得的质子物质的拉曼信号似乎与它们的年代相关，但是也应该考虑其他因素，例如影响腐蚀程度的机械损伤（裂纹、空隙）。

3.6 | Porcelains |陶瓷

3.6.1 | Glazes | 釉料

The wave-corrected Raman spectra of the porcelains are given in Figure 8, left. The spectrum of the Ming porcelain (M-blb; blue underglaze decor, the colourless glaze being fired with the porcelain body) particularly represents a rather strong Raman signature of the protonic species (~2,700 and 2,900 cm −1 for H-bonded species and ~3,180 cm −1 for water; Table 3; Figure 8b, left).
陶瓷的波修正拉曼光谱如图8（左图）所示。明代陶瓷的光谱（M-blb；釉下青花装饰，无色釉与瓷体一起烧制）尤其显示出质子物质相当强的拉曼信号（氢键结合物质约为2700和2900cm-1，水约为3180cm-1；表3图8b，左图）。

The fake porcelain (F-p) and the other Ming porcelain (M-blc) show different Raman signatures with the features at 2,850 and 3,730 cm −1, which result from the H-bonded species and hydroxyl groups, respectively (Figure 8d,e, left). In these spectra, fluorescence is also observed in the region 3,000–3,500 cm −1. In the case of sample F-p, it should be noted that defects might have been made in the glaze to mimic an old appearance, but it is not known whether some treatments have been made to “age” the object.

陶瓷仿制品（F-p）和其他明代陶瓷（M-blc）表现出不同的拉曼信号，分别为2850和3730 cm-1处，分别表示氢键物质和羟基（图8d，e，左图）。在这些光谱中，在3,000–3,500 cm-1处也观察到了荧光。就样品F-p而言，需要注意的是，为了模仿旧的外观，釉料中可能会存在缺陷，但不知道是否进行了某些技术处理来“做旧”该物品。

3.6.2 | Lead‐based overglazes |铅基釉

The spectrum of the green lead-based overglaze of the Qing Famille Rose porcelain (Q-r) displays a very strong Raman signature of the protonic species, with ~2,700 and ~2,900 cm −1 for H-bonded species and ~3,180 cm −1 for water (Table 3; Figure 8a, left). The spectrum of the other green lead-based overglaze of the Qing wucai porcelain (Q- bl) displays a well-distinguished band at 2,920 cm −1, which is due to the H-bonded species (Table 3; Figure 8f, left) whereas the green enamel of the Qing painted porcelain (Q-p) has a lower intensity signal but displays an additional peak at 3,560 cm −1, which is assigned to the hydroxyl groups (Figure 8c, left). This peak seems to be characteristic of the corroded lead-based glaze.

清代粉彩瓷（Q-r）绿色铅基釉的光谱显示质子物质的拉曼信号非常强，氢键物质的拉曼信号约为2,700和2,900cm-1，水的拉曼信号约为3,180cm-1（表3；图8a，左图）。清代五彩瓷器（Q-bl）的另一种绿色铅基釉的光谱在2,920cm-1处显示出非常明显的谱带，这是氢键结合物质造成的（表3；图8f，左侧），而清代彩瓷（Q-p）的绿瓷釉具有较低的强度信号，但在3,560cm-1处显示附加峰值，该峰值表示羟基（图8c，左图）。该峰值表明存在受到腐蚀的铅基釉料。

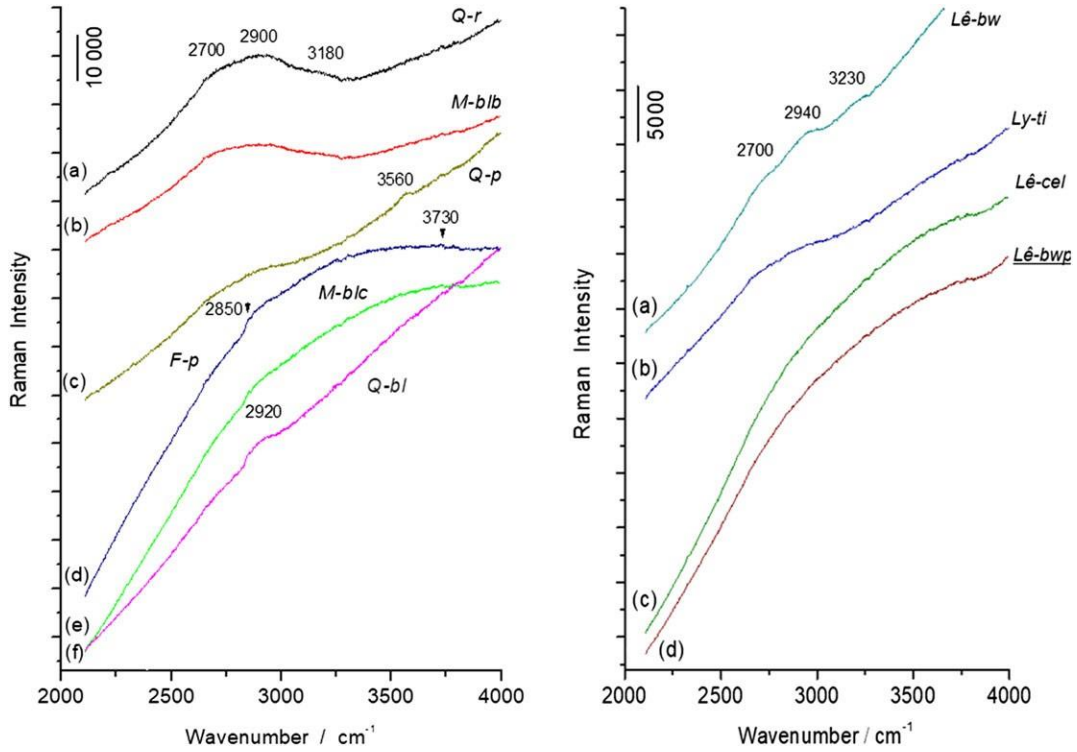


FIGURE 8 Representative wave‐corrected Raman spectra recorded on Qing and Ming Dynasty (over) glazed porcelains (left) and Vietnamese porcelains or celadons excavated or from shipwreck (right; ×100 objective; c.h.: 200 μm; see Table 1 for more details) [Colour figure can be viewed at wileyonlinelibrary.com]
图8 清朝和明朝（上图）釉瓷（左图）和挖掘或沉船中的越南瓷器或青瓷的代表性波修正拉曼光谱（右图；×100物镜；c.h.:200μm；详见表1） [彩图请浏览wileyonlinelibrary.com]

3.7 | Samples excavated or recovered from shipwreck

3.7 |从沉船中挖掘或回收的样品

Figure 8, right compares the wave-corrected Raman spectra of the Vietnamese porcelains or celadons either being excavated from kilns or recovered from the Cu Lao Cham shipwreck. The shipwreck samples are expected to have been exposed to more active corrosion conditions as a result of their long term stay in sea water. The spectrum of the porcelain sample from the 15th century shipwreck (Lê-bw) displays bands at 2,700, 2,940, and 3,230 cm −1, which are assigned to H-bonded species and water, respectively (Table 3; Figure 8a, right). The other samples show different types of Raman spectra with varying intensities (Figure 8b–d, right). Consequently, it can be proposed for the last sample categories that the composition of the glazes and the environmental conditions are other factors to be considered affecting the Raman signature of the protonic species apart from the age.

图8比较了从窑中挖掘或从Cu Lao Cham沉船中回收的越南瓷器或青瓷的波修正拉曼光谱。沉船样品由于长期置于海水中，预计会暴露于更活跃的腐蚀条件下。15世纪沉船出土的瓷器样品的光谱显示了2,700、2,940和3,230cm-1处的谱带，分别表示氢键物质和水（表3；图8a，右图）。其他样品显示不同强度下不同类型的拉曼光谱（图8b-d，右图）。因此，对于最后的样品类别，可以得出结论，除年龄之外，釉料的成分和环境条件是影响质子物质拉曼信号的其他因素。

4 | DISCUSSION

|讨论

As mentioned before, the Raman intensity obtained is directly related to the optical properties of the materials analysed because Raman spectroscopy is an optical technique.
如上所述，因为拉曼光谱技术是一种光学技术，所以获得的拉曼强度与所分析材料的光学性质直接相关。

The absolute Raman intensity of the silicate signature was found to be an effective tool in the discrimination of similar types of glasses as a function of time according to their varying degrees of corrosion, which in turn affect the transparency of glass. [6,17] The relative intensity of the Raman signature of protonic species incorporated in the glassy silicate network on the glass or glaze surface was also previously proposed as a potential tool for the discrimination of artefacts (kept in the same conditions) as a function of age. [16] The results of our analyses on different types of glazed pottery samples showed that there is a correlation between the relative intensity of the broad Raman signature of the protonic species and the age of the artefact to a certain degree including the celadon or stoneware and porcelain samples. For the comparison of all the data obtained, a plot of the so-called H 2O/OH band area as an indicator of Raman intensity of the protonic species versus elapsed time since production date was drawn where Y scale is logarithmic and X scale is taken as inverse time (assuming an Arrhenius law for the diffusion of the protonic species in the glass), [11] including the regression lines for the sample groups (Figure 9). The band area was mostly calculated between the wavenumbers ~2,300 to ~3,300 cm −1 with variations in some of the spectra according to the shape of the spectrum.

研究发现，硅酸盐特征的绝对拉曼强度是用于根据相似类型的玻璃的不同腐蚀程度来区分随时间变化的相似类型玻璃的有效工具，反过来又影响玻璃的透明度。[6，17]玻璃或釉面玻璃硅酸盐网络中质子物质的拉曼信号相对强度也曾被提议作为辨别受年龄影响的手工艺品（保持在相同条件下）的潜在工具。[16]我们对不同类型釉陶样品的分析结果表明，包括青瓷或炻瓷、瓷器样品在内的质子物质的宽拉曼信号的相对强度与手工艺品的年龄之间在一定程度上存在相关性。为了比较所有获得的数据，绘制了作为质子物质拉曼强度指标的所谓H 2O/OH谱带面积与自生产日期以来的时间曲线图，其中Y标度指对数，而X标度是反向时间（假设质子物质在玻璃中扩散符合阿伦尼乌斯

定律），[11]包括样品组的回归线（图9）。主要计算波数约 2,300至约3,300cm-1处之间的谱带面积，根据光谱的形状，某些光谱会有变化。

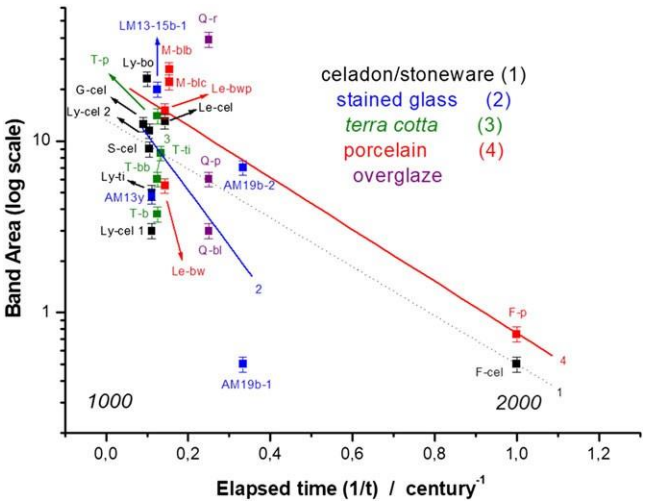


FIGURE 9 H_2O/OH band area vs. time elapsed since production date for celadons or stoneware, reference stained glasses, glazed *terra cottas*, porcelains, and porcelain overglazes. Regression lines are given indicating the groups. (±10% error bars are included) [Colour figure can be viewed at wileyonlinelibrary.com]
图9 青瓷或炻瓷、参考彩色玻璃、釉陶、瓷器和瓷釉的H 2O/OH带面积与自生产日期以来经过的时间的关系。给出的回归线表示各组。（包括10 %误差线） [彩图请浏览wileyonlinelibrary.com]

The more or less fluorescent background leads to some uncertainty in the measurement of the band area. The band area was calculated for each spectrum using the blocks of the graduated paper by visual examination (the procedure is described in more detail in Figure S2). The fitting lines were determined by Origin 6.0 software tool using a linear regression analysis. It should be noted that the error of area measurement is considered to be mostly about ±10%.

或多或少的荧光背景会导致谱带面积测量出现偏差。通过目检，使用刻度纸块计算每个光谱的谱带面积（详细程序请见图S2）。通过Origin 6.0软件工具使用线性回归分析确定了拟合线。应注意的是，我们认为面积测量误差约为10 %。

In Figure 9, we observe a similar slope for the glazes of celadons or stoneware and porcelains, lower than that of stained glasses. With this mathematical representation used, the band area depends exponentially on the inverse of elapsed time and the slope of the fitting line is similar to the activation energy, as in the case of the expression of ion diffusion versus time following the Arrhenius rule. Rather similar activation energy is thus observed for the glazes of celadons or stoneware and porcelains whereas a much higher one is the case for stained glasses. It was not possible to determine the parameter according to the linear regression analysis for the terra cotta glazes due to the lack of similar modern samples. However, when the data for the terra cotta glazes and the porcelain overglazes are considered together in linear regression analysis, the slope (activation energy) of the fitting line is even higher than that of stained glasses, making the fitting line almost horizontal. Thus, we can strongly suggest that these observations are consistent with the chemical composition of the glazes in the regarding sample groups. In the case of stained glasses, the potash-based composition makes them less resistant to corrosion due to the easy exchange of K + ions with H + and/or H 3O + ions. [8] However, the celadons or stoneware and porcelain samples include glazes with a higher durability due to their lime- and feldspar-based composition (i.e., “alumina-rich”), making them corrode relatively slower than stained glasses.

在图9中，我们发现青瓷或炻瓷和瓷器的釉料斜率相似，比彩色玻璃的斜率要低。使用这种数学表达式，谱带面积指数取决于经过时间的倒数，拟合线的斜率类似于活化能，正如遵循阿伦尼乌斯定律的离子扩散对时间的表达式的情况。因此，在青瓷或炻瓷和瓷器的釉料中发现的活化能相当相似，而彩色玻璃的活化能则要高得多。由于缺少类似的现代样品，无法根据釉陶的线性回归分析来确定参数。然而，当在线性回归分析中将釉陶数据和瓷釉数据放在一起考虑时，拟合线的斜率（活化能）甚至高于彩色玻璃的斜率，使得拟合线几乎呈水平。因此，我们坚定地认为这些观察结果与相关样品组中釉料的化学成分一致。对于彩色玻璃，由于钾基组合物中的钾离子容易与氢离子和/或H3O +离子交换，使得其耐腐蚀性较差。[8]但青瓷或炻瓷和瓷器样品的釉料具有更好的耐久性，这是因为它们的石灰和长石成分（即“富含氧化铝”）使得它们的腐蚀速度相对低于彩色玻璃。

On the other hand, the effect of chemical composition is very dominant in the cases of lead-based terra cotta glazes and porcelain overglazes concerning the amount of lead which increases the reactivity of the glaze and make them the most corroded. As a result, the correlation between elapsed time (age) and Raman intensity is mostly valid for the sample groups that are the most resistant to corrosion. However, it is also clear that more data are necessary to build up the empirical law concerning the “H 2O/OH” band area as a possible dating tool. It should also be noted that spectra from each sample were recorded on three spots in this study, and the most representative one was used for the area calculation. Obviously, a statistical approach could improve the efficiency of the method, especially if only one type of object is studied.

另一方面，对于铅釉陶和瓷釉，化学成分的影响非常显著，铅的含量增加了釉料的反应性，使其腐蚀情况最严重。因此，经过时间（年龄）和拉曼强度之间的相关性对于最耐腐蚀的样品组来说最为适用。然而，这显然需要更多的数据来建立关于“H 2O/OH”谱带面积的经验法则，来作为可能使用的定年工具。还应注意的是，在本研究中，将每个样品的光谱记录在三个点上，使用最具代表性的一个点来计算面积。显然，统计方式可提高该方法的效率，特别是在只研究一种类型对象的情况下。

Figure S3 shows the as-recorded and wave-corrected Raman spectra of the Qing Famille Rose porcelain sample (Q-r) obtained from preliminary measurements performed on the section of shards at different distances from the glaze surface in the high wavenumber region. [16,26] Unfortunately, in this preliminary work, the selected wavenumber window (3,000–3,800 cm −1) being too small hinders the clear observation of all the components. However, the measurements show very well that the intensity is relatively stronger at ~3,170 cm −1, just at the limit of the window in the spectrum, which is the closest one to the surface (Figure S3, left). This is due to the fact that the corrosion phenomenon is initiated at the very surface of glass due to the presence of protonic species resulting in the formation of a corrosion layer (hydration layer). As expected, the more distant spectrum represents almost no signal of the protonic species. In the case of focusing towards the inner structure of glaze, the signal of the protonic species is lost due to the limited thickness of the corroded layer (see also Figure S4 for the low wavenumber region from the glaze towards the paste). It is thus important to use a high magnification microscope objective (×100 or ×200) and to focus the spot precisely at the very surface of the sample.

图S3显示了清代彩釉瓷器样品（Q-r）的记录和波修正拉曼光谱，产生该光谱的方式是对高波数区釉面不同距离的碎片部分进行初步测量。[16，26]不幸的是，在这项初步工作中，由于选定的波数窗口（3，000–3，800 cm −1）太小，未能清晰观察所有成分。但测量清楚表明，3，170 cm −1左右处的强度相对较强，恰好在光谱窗口的极限处，该窗口与表面最接近（图S3，左侧）。这是由于质子物质导致腐蚀层（水合层）形成，而腐蚀现象一开始出现于玻璃的最表面。不出所料，更远的光谱几乎不存在质子物质信号。如果聚焦于釉料内部结构，质子物质信号会由于腐蚀层的有限厚度而丢失（参见图S4，以了解从釉料到糊料的低波数区域）。因此，必须使用高放大倍数的显微镜物镜（×100或×200）并将束斑精确聚焦在样品的表面。

5 | CONCLUSION
结论

In this study, the possibility of a comparative dating or authentication procedure on the basis of the Raman signature of protonic species accumulated at the surface of glass or glaze is investigated for the first time by using a selection of glazed pottery samples from different origins and time periods (from ca. 11th century up to the present time).

在本研究中，通过选择不同来源和时间周期的釉陶样品，首次研究了根据积累在玻璃或釉料上的质子物质的拉曼信号进行比较定年或鉴定的可能性（从11世纪至今）。

As in the case of the absolute Raman intensity collected from similar types of glasses with varying degrees of corrosion, the evaluation of the relative Raman intensity of the protonic species signature at the sample surface proved to be useful as a means of comparative dating or authentication especially for celadons or stoneware and porcelain samples, which have a lead free chemical composition. The modern fakes can also be identified by no visible signature of protonic species but a fluorescence signal. We can conclude that the information about the age of glazed pottery can be obtained by this procedure depending strongly on the glaze composition and weakly on the environmental conditions of preservation. The method appears to be more appropriate to detect fakes than to provide an accurate dating; thus, it can specifically be proposed as a fast and non-invasive method for the discrimination between old and modern artefacts (copies or fakes) in terms of authentication. Additionally, the efficiency of the method will be strengthened with the integration of more data collected from very similar objects.

如同从不同腐蚀程度的类似类型玻璃收集的绝对拉曼强度的情况一样，经证实，对样品表面质子物质特征的相对拉曼强度进行评估，可作为比较定年或鉴定的手段，特别是对于含无铅化学成分的青瓷或炻瓷和瓷器样品。同样，如果未发现质子物质特征但发现荧光信号，则可判定为现代仿制品。我们认为，可以通过这一程序获知釉陶的年代信息，其主要取决于釉料成分，保存的环境条件则次要。这种方法似乎更适合检测仿制品，而非进行准确定年；因此，其可作为专门鉴别新旧手工艺品（复制品或仿制品）的快速和非侵入性方法。此外，整合相似对象的更多收集数据可提高该方法的效率。

ACKNOWLEDGEMENTS
致谢

Dr. Céline Paris is kindly acknowledged for her advices in the recording of the Raman spectra. Mr. Lee Koon Keung and Li Kong Lung from Royal Heritage Ceramics Authentication Ltd. are also acknowledged for many discussions, the incitation to make this study, and partial support.

感谢Céline Paris博士在拉曼光谱记录方面提出的建议。也感谢皇朝遗珍古陶瓷实验室的李灌强先生和李港龙先生为本研究进行多次讨论、给予鼓励和部分支持。

ORCID
ORCID

Philippe Colomban https://orcid.org/0000-0001-6099-5423
Philippe Colomban https://orcid.org/0000-0001-6099-5423

REFERENCES
参考文献

[1] R. H. Brill, H. P. Hood, *Nature* **1961**, *189*(4758), 12.
[1]R. H. Brill, H. P. Hood, Nature 1961, 189(4758), 12.
[2] R. H. Doremus, *J. Non‐Cryst. Solids* **1975**, *19*, 137.
R. H. Doremus, J. Non‐Cryst.Solids 1975，19，137。
[3] M. Perez y Jorba, J. P. Dallas, C. Bauer, C. Bahezre, J. C. Martin, *J. Mater. Sci.* **1980**, *15*(7), 1640.
M. Perez y Jorba, J. P. Dallas, C. Bauer, C. Bahezre, J. C. Martin, J. Mater.*Sci.***1980**, *15*(7), 1640.
[4] W. A. Lanford, K. Davis, P. Lamarche, T. Laursen, R. Groleau, R. H. Doremus, *J. Non‐Cryst. Solids* **1979**, *33*(2), 249. [5] G. A. Cox, B. A. Ford, *J. Mater. Sci.* **1993**, *28*(20), 5637.
W. A. Lanford, K. Davis, P. Lamarche, T. Laursen, R. Groleau, R. H. Doremus, J. Non‐Cryst.Solids 1979，33（2），249。[5] G. A. Cox, B. A. Ford, J. Mater。*Sci.***1993**, *28*(20), 5637.
[6] P. Colomban, A. Tournié, *J. Cult. Herit.* **2007**, *8*(3), 242.
P. Colomban, A. Tournié, J. Cult。*Herit.***2007**, *8*(3), 242.
[7] M. Vilarigues, R. C. da Silva, *J. Non‐Cryst. Solids* **2006**, *352*(50–51), 5368.
M. Vilarigues, R. C. da Silva, J. Non‐Cryst.Solids 2006，352（50–51），5368。
[8] A. Tournié, P. Ricciardi, P. Colomban, *Solid State Ionics* **2008**, *179*(38), 2142.
A. Tournié，P. Ricciardi，P. Colomban，Solid State Ionics 2008，179（38），2142。
[9] P. Colomban, *J. Mater. Sci.* **1989**, *24*(8), 3011.
[9]P. Colomban, J. Mater.*Sci.***1989**, *24*(8), 3011.
[10] V. Vendange, P. Colomban, *J. Porous Mater.* **1996**, *3*(3), 193.
V. Vendange, P. Colomban, J. Porous Mater.**1996**, *3*(3), 193.
[11] P. Colomban, A. Novak, Proton Conductors Solids, Membranes and Gels‐Materials and Devices, in , (Ed: P. Colomban), Cambridge University Press, Cambridge **1992** 272.
P. Colomban, A. Novak, Proton Conductors Solids, Membranes and Gels‐Materials and Devices, in,(Ed:P.Colomban), Cambridge University Press, Cambridge 1992 272.
[12] T. Calligaro, Y. Coquinot, I. Reiche, J. Castaing, J. Salomon, G.
T. Calligaro，Y. Coquinot，I. Reiche，J. Castaing，J. Salomon，g .
Ferrand, Y. Le Fur, *Appl. Phys. A* **2009**, *94*(4), 871.
Ferrand, Y. Le Fur, Appl.*Phys.*A 2009, 94(4), 871.
[13] I. Friedman, R. L. Smith, *Science* **1959**, *129*(3358), 1285.
[13]I. Friedman, R. L. Smith, Science 1959, 129(3358), 1285.
[14] J. E. Ericson, O. Dersch, F. Rauch, *J. Archaeol. Sci.* **2004**, *31*(7), 883.
J. E. Ericson, O. Dersch, F. Rauch, J. Archaeol.*Sci.***2004**, *31*(7), 883.
[15] P. Ricciardi, P. Colomban, A. Tournié, V. Milande, *J. Raman Spectrosc.* **2009**, *40*(6), 604.
P. Ricciardi, P. Colomban, A. Tournié, V. Milande, J. Raman Spectrosc.**2009**, *40*(6), 604.
[16] P. Colomban, *J. Raman Spectrosc.* **2018**, *49*(6), 921.
P. Colomban, J. Raman Spectrosc.**2018**, *49*(6), 921.
[17] D. Mancini, A. Tournié, M.‐C. Caggiani, P. Colomban, *J. Raman Spectrosc.* **2012**, *43*(2), 294.
D. Mancini, A. Tournié, M.‐C. Caggiani, P. Colomban, J. Raman Spectrosc.**2012**, *43*(2), 294.
[18] N. Q. Liem, N. T. Thanh, P. Colomban, *J. Raman Spectrosc.*
N. Q. Liem, N. T. Thanh, P. Colomban, J. Raman Spectrosc.
2002, *33*(4), 287.
2002, *33*(4), 287.
[19] G. Gouadec, P. Colomban, *Prog. Cryst. Growth Charact. Mater.*
G. Gouadec, P. Colomban, Prog.*Cryst.Growth Charact.Mater.*
2007, *53*(1), 1.
2007, *53*(1), 1.
[20] P. Colomban, *Fuel Cells* **2013**, *13*(1), 6.
P. Colomban, Fuel Cells 2013, 13(1), 6.
[21] G. Li, H. Ji, C. Lv, N. Li, Y. Hong, L. Zhang, *J. Non‐Cryst. Solids* **2019**, *505*, 102.
G. Li, H. Ji, C. Lv, N. Li, Y. Hong, L. Zhang, J. Non‐Cryst.Solids 2019，505，102。
[22] P. Colomban, M.‐P. Etcheverry, M. Asquier, M. Bounichou, A. Tournié, *J. Raman Spectrosc.* **2006**, *37*(5), 614.
P. Colomban, M.‐P. Etcheverry, M. Asquier, M. Bounichou, A. Tournié, J. Raman Spectrosc.**2006**, *37*(5), 614.
[23] G. Şimşek, P. Colomban, S. Wong, B. Zhao, A. Rougeulle, N. Q. Liem, *J. Cult. Herit.* **2015**, *16*(2), 159.
G. Şimşek, P. Colomban, S. Wong, B. Zhao, A. Rougeulle, N. Q. Liem, J. Cult.*Herit.***2015**, *16*(2), 159.
[24] Z. Fukang, Ancient Technology to Modern Science, Ceramics and Civilization vol. 1, in , (Ed: W. D. Kingery), The American Ceramic Society, Columbus **1984** 163.
Z. Fukang, Ancient Technology to Modern Science, Ceramics and Civilization vol. 1, in,(Ed:W.D. Kingery), The American Ceramic Society, Columbus 1984 163.
[25] Y. Qu, J. Xu, X. Xi, C. Huang, J. Yang, *Ceram. Int.* **2014**, *40*(6), 8783.
Y. Qu, J. Xu, X. Xi, C. Huang, J. Yang, Ceram.Int. 2014, 40(6), 8783.

[26] P. Colomban, F. Ambrosi, A. - T. Ngo, T. - A. Lu, X. - L. Feng, S. Chen, C. - L. Choi, *Ceram. Int.* **2017**, *43*(16), 14244.
P. Colomban, F. Ambrosi, A. - T. Ngo, T. - A. Lu, X. - L. Feng, S. Chen, C. - L. Choi, Ceram.Int. 2017, 43(16), 14244.
[27] P. Colomban, N. Q. Liem, G. Sagon, H. X. Tinh, T. B. Hoanh, *J. Cult. Herit.* **2003**, *4*(3), 187.
P. Colomban, N. Q. Liem, G. Sagon, H. X. Tinh, T. B. Hoanh, J. Cult.*Herit.***2003**, *4*(3), 187.
[28] J. N. Miksic, Southeast Asian Ceramics: New Light on Old Pottery, in , (Ed: J. N. Miksic), Southeast Asian Ceramic Society, Singapore **2009** 58.
J. N. Miksic, Southeast Asian Ceramics:New Light on Old Pottery, in,(Ed:J.N. Miksic), Southeast Asian Ceramic Society, Singapore 2009 58.
[29] B. M. Tri, T. T. Tin, N. Q. Liem, P. Colomban, *Taoci* **2001**, *2*, 105.
B. M. Tri, T. T. Tin, N. Q. Liem, P. Colomban, Taoci 2001, 2, 105.
[30] N. Q. Liem, G. Sagon, V. X. Quang, H. V. Tan, P. Colomban, *J. Raman Spectrosc.* **2000**, *31*(10), 933.
N. Q. Liem, G. Sagon, V. X. Quang, H. V. Tan, P. Colomban, J. Raman Spectrosc.**2000**, *31*(10), 933.
[31] N. Wood, *Chinese Glazes: Their Origins, Chemistry and Recreation*, University of Pennsylvania Press, Philadelphia **1999**.
N. Wood, Chinese Glazes:Their Origins, Chemistry and Recreation, University of Pennsylvania Press, Philadelphia 1999.
[32] P. Colomban, C. Truong, *J. Raman Spectrosc.* **2004**, *35*(3), 195.
P. Colomban, C. Truong, J. Raman Spectrosc.**2004**, *35*(3), 195.
[33] P. Colomban, G. Sagon, A. Louhichi, H. Binous, N. Ayed, *R. Archeom.* **2001**, *25*(1), 101.
P. Colomban, G. Sagon, A. Louhichi, H. Binous, N. Ayed, R. Archeom.**2001**, *25*(1), 101.
[34] P. Colomban, *Appl. Phys. A* **2004**, *79*(2), 167.
[34]P. Colomban, Appl.*Phys.*A 2004, 79(2), 167.
[35] D. Hadzi, *Pure Appl. Chem.* **1965**, *11*(3–4).
D. Hadzi, Pure Appl.*Chem.***1965**, *11*(3–4).
[36] D. Hadzi, S. Bratos, The Hydrogen Bond Recent Developments in Theory and Experiments, in , (Eds: P. Schuster, G. Zundel, C. Sandorfy), North Holland Publishing Co., Amsterdam **1976** Chapt. 2.
D. Hadzi, S. Bratos, The Hydrogen Bond Recent Developments in Theory and Experiments, in,(Eds:P.Schuster, G. Zundel, C. Sandorfy), North Holland Publishing Co., Amsterdam 1976 Chapt. 2.
[37] P. Colomban, *J. Mol. Struct.* **1992**, *270*, 407.
P. Colomban, J. Mol.*Struct.***1992**, *270*, 407.
[38] A. Slodczyk, P. Colomban, S. Willemin, O. Lacroix, B. Sala, *J. Raman Spectrosc.* **2009**, *40*(5), 513.
A. Slodczyk, P. Colomban, S. Willemin, O. Lacroix, B. Sala, J. Raman Spectrosc.**2009**, *40*(5), 513.

[39] P. Colomban, A. Tournié, L. Bellot‐Gurlet, *J. Raman Spectrosc.* P. Colomban, A. Tournié, L. Bellot‐Gurlet, J. Raman Spectrosc. **2006**, *37*(8), 841.
2006, *37*(8), 841.
[40] M. Havel, P. Colomban, *Spectrosc. Eur. Microsc. Anal.* **2006**, *20*(3), 13.
M. Havel, P. Colomban, Spectrosc.*Eur.Microsc.Anal.***2006**, *20*(3), 13.
[41] M. L. Frezzotti, F. Tecce, A. Casagli, *J. Geochem. Explor.* **2012**, *112*, 1.
M. L. Frezzotti, F. Tecce, A. Casagli, J. Geochem.*Explor.***2012**, *112*, 1.
[42] P. Colomban, L. C. Prinsloo, Spectroscopic Properties of Inorganic and Organometallic Compounds: vol 40, in , (Eds: J. Yarwood, R. Douthwaite, S. Duckett), The Royal Society of Chemistry, Cambridge **2009** 128.
P. Colomban, L. C. Prinsloo, Spectroscopic Properties of Inorganic and Organometallic Compounds:vol 40, in,(Eds:J.Yarwood, R. Douthwaite, S. Duckett), The Royal Society of Chemistry, Cambridge 2009 128.
[43] P. Colomban, Modern Methods for Analysing Archaeological and Historical Glass, in , 1st ed. (Ed: K. H. A. Janssens), John Wiley & Sons Ltd, India **2013** 275.
P. Colomban, Modern Methods for Analysing Archaeological and Historical Glass, in, 1st ed.(Ed:K.H. A. Janssens), John Wiley&Sons Ltd, India 2013 275.
[44] P. Colomban, Analytical Archaeometry: Selected Topics, in , (Eds: H. G. M. Edwards, P. Vandenabeele), The Royal Society of Chemistry, Cambridge **2012** 245.
P. Colomban, Analytical Archaeometry:Selected Topics, in,(Eds:H.G. M. Edwards, P. Vandenabeele), The Royal Society of Chemistry, Cambridge 2012 245.
[45] P. Colomban, *J. Non‐Cryst. Solids* **2003**, *323*(1–3), 180.
P. Colomban, J. Non‐Cryst.*Solids* **2003**, *323*(1–3), 180.
[46] P. Colomban, O. Paulsen, *J. Am. Ceram. Soc.* **2005**, *88*(2), 390.
P. Colomban, O. Paulsen, J. Am. Ceram.*Soc.***2005**, *88*(2), 390.
[47] V. Labet, P. Colomban, *J. Non‐Cryst. Solids* **2013**, *370*(15), 10.
V. Labet, P. Colomban, J. Non‐Cryst.Solids 2013, 370(15), 10.
[48] R. A. Eppler, D. R. Eppler, *Glazes and Glass Coatings*, The American Ceramic Society, Westerville **2000**.
R. A. Eppler, D. R. Eppler, Glazes and Glass Coatings, The American Ceramic Society, Westerville 2000.
[49]
[50] J. Zarzycki, *Glasses and The Vitreous State Cambridge Solid State Science Series*, Cambridge University Press, Cambridge **1991**.
J. Zarzycki, Glasses and The Vitreous State Cambridge Solid State Science Series, Cambridge University Press, Cambridge 1991.
[51] C. Bonnet, A. Bouquillon, S. Turrell, V. Deram, B. Mille, J. Salomon, J. H. Thomassin, C. Fiaud, *J. Non‐Cryst. Solids* **2003**, *323*(1–3), 214.
C. Bonnet, A. Bouquillon, S. Turrell, V. Deram, B. Mille, J. Salomon, J. H. Thomassin, C. Fiaud, J. Non‐Cryst.*Solids* **2003**, *323*(1–3), 214.

SUPPORTING INFORMATION
支持信息

Additional supporting information may be found online in the Supporting Information section at the end of the article.
更多支持信息可通过网络浏览论文末尾的“支持信息”部分。

本文引用方式： Kırmızı B, Chen S, Colomban P. 釉陶定年或鉴定潜在工具——质子物质的拉曼信号。J Raman Spectrosc.2019;1–15.https://doi.org/10.1002/ jrs.5558